NASA Technical Memorandum

NASA TM -86530

AURORAL THERMOSPHERE TEMPERATURES FROM OBSERVATIONS OF 6300 Å EMISSIONS

By John C. Bird, Gary R. Swenson, and
Richard H. Comfort

Space Science Laboratory
Science and Engineering Directorate

(NASA-TM-86530) AURORAL THERMOSPHERE TEMPERATURES FROM OBSERVATIONS OF 6300 A EMISSIONS (NASA) 65 p HC A04/MF A01 N86-15755
CSCL 04A Unclas
G3/46 05036

November 1985

NASA
National Aeronautics and
Space Administration
George C. Marshall Space Flight Center

TECHNICAL REPORT STANDARD TITLE PAGE

1. REPORT NO. NASA TM- 86530	2. GOVERNMENT ACCESSION NO.	3. RECIPIENT'S CATALOG NO.
4. TITLE AND SUBTITLE Auroral Thermosphere Temperatures from Observations of 6300 Å Emissions		5. REPORT DATE November 1985
		6. PERFORMING ORGANIZATION CODE ES53
7. AUTHOR(S) John C. Bird,*+ Gary R. Swenson,++ and Richard H. Comfort**		8. PERFORMING ORGANIZATION REPORT #
9. PERFORMING ORGANIZATION NAME AND ADDRESS George C. Marshall Space Flight Center Marshall Space Flight Center, Alabama 35812		10. WORK UNIT NO.
		11. CONTRACT OR GRANT NO.
		13. TYPE OF REPORT & PERIOD COVERED Technical Memorandum
12. SPONSORING AGENCY NAME AND ADDRESS National Aeronautics and Space Administration Washington, D.C. 20546		
		14. SPONSORING AGENCY CODE

15. SUPPLEMENTARY NOTES

Prepared by Space Science Laboratory, Science and Engineering Directorate

*Department of Mechanical Engineering, The University of Alabama, Huntsville

**Department of Physics, The University of Alabama, Huntsville

16. ABSTRACT

Doppler temperatures determined from observations of the atomic oxygen OI 6300 Å line during March 1984 at the University of Alaska/Fairbanks are presented. Temperatures were obtained from Fabry-Perot Interferometer pressure scans using a Fourier transform smoothing and fitting technique; this technique is presented in detail. The temperatures and the spread in the temperatures were consistent from day to day. On the clear nights of March 10-13, the temperatures were 800, 750, 750, and 800 K, respectively, with a spread of ±100 K. These temperatures are compared to the MSIS (84) model atmosphere for similar geomagnetic conditions and found to be in general agreement; they are also consistent with results obtained by other investigators.

+Now at York University, Toronto, Canada

++Now at Lockheed Missiles and Space Company, Inc., Palo Alto, California

17. KEY WORDS Fabry-Perot Interferometer Thermosphere Temperatures Auroral Thermosphere	18. DISTRIBUTION STATEMENT Unclassified - Unlimited

19. SECURITY CLASSIF. (of this report) Unclassified	20. SECURITY CLASSIF. (of this page) Unclassified	21. NO. OF PAGES 66	22. PRICE NTIS

MSFC - Form 3292 (May 1969)

For sale by National Technical Information Service, Springfield, Virginia 22151

TABLE OF CONTENTS

PRECEDING PAGE BLANK NOT FILMED

LIST OF ILLUSTRATIONS

I. INTRODUCTION

This report summarizes the results of a set of observations of the atomic oxygen OI 15,867 K 6300 Å $^3P-^1D$ thermospheric emission to determine the temperature of the emitting species using a Fabry-Perot interferometer at the University of Alaska Geophysical Institute (64.86° latitude, -147.85° longitude) during March 1984. Spectral profiles obtained from the interferometer are used to determine the Doppler temperature by means of the technique reported by Hays and Roble [1] and Roble [2].

This general concept of using Doppler widths of airglow lines to find temperatures has been used by many investigators such as Wark [3], Nilson and Shepherd [4], Turgeon et al. [5], Zwick and Shepherd [6], Hernandez [7], Hernandez and Roble [8-11], and Smith et al. [12]. Analytical descriptions of Fabry-Perot spectrometers have been presented by Born and Wolfe [13] and Hernandez [14]. A review of temperatures and winds measured by Fabry-Perot spectrometry was done by Hernandez [7].

II. INSTRUMENTATION

The Fabry-Perot interferometer was located on the top floor of the Geophysical Institute, Fairbanks, Alaska, allowing observations through a variable geometry periscope system and a Plexiglass dome. The interferometer is described by Roble [2] and Sivjee et al. [15] and is shown in Figures 1 and 3. Spectral profiles were obtained by pressure scanning of the etalon in steps. A stepper motor controlled the piston (shown in Figure 2), and position data were provided by an A/D encoder. During a pressure scan, the refractive index in the etalon changed. This caused the light in the center of the interferometer pattern to change intensity, creating an intensity/pressure fringe. This light from the interferometer was reflected through a 1/8-inch aperture, then filtered, and finally detected by a photomultiplier tube. Simultaneously, a photometer recorded the intensity of the 6300 Å lines in the same direction as the interferometer observation. Also, the etalon temperature was monitored. Pressure scanning, mirror positioning, and integration times were controlled by computer. Times, pressures, observation directions, temperatures, and counts were automatically stored in the format shown in Appendix F.

An He-Ne (6328 Å) frequency-stabilized Tropel laser was used for calibration. To prevent photomultiplier tube saturation, the beam was incident on a ground glass sphere above the interferometer. The glowing sphere simulated the sky, so pressure scanning produced fringes without changing the experimental setup from the sky observation configuration. If, during calibration, the fringes were found to be asymmetric, the aperture or, in extreme cases, the etalon plates were adjusted. Neither of these adjustments were required between the observations included in this report, although such adjustments were required between earlier trial runs.

III. OBSERVATIONS

Observations were made at an inclination of 30° from the horizontal in the north, south, east, and west magnetic directions. Observations were also made at local zenith. All observations were made between sunset and sunrise from March 6 to March 16, 1984. At the beginning of this period the moon was only 9% full; but by March 16, it was 97% full.

Most nights were clear, and slight to moderate auroral activity was observed in the zenith and to the north. On clear nights, diffuse aurorae were usually seen to the north. Data were also taken on cloudy and foggy nights, even though the observed light was scattered from all sky sources prior to detection. If there is mass average velocity with the emitting atoms, the temperature measurement is still correct. Winds could cause an error if they were unusually strong under these cloudy conditions.

In addition, the raw data were monitored during all runs. For example, an X-Y plotter was used to record the intensity of the interferometer image as a function of pressure to monitor the fringes and to provide a quick look at the raw data. After each night of observations, the records stored in the computer were transferred to disks. The parameters that were monitored and the formatting of this data are discussed in the following section.

IV. DATA REDUCTION

The computer program for data analysis included: reading of data from disk, temperature and pressure compensations, normalization, Fourier transform smoothing, deconvolution, and least squares fitting to theoretical profiles. A listing of this program is included in Appendix D along with a sample output.

A. Data Format, Reading Data

Each pressure scan of 64 steps included one free spectral range or fringe, which covered only 34 steps. The other 30 steps corresponded to other fringes and were, therefore, ignored. These fringes occurred as variations in photomultiplier counts as functions of pressure. Data at each step included etalon pressure and temperature, photometer reading, and photomultiplier reading. Times were recorded at the beginning of each pressure scan. All these data were stored in files such as the one shown in Appendix F. The first step in the data analysis program was to read the data corresponding to one fringe.

B. Data Modification

First, the reading of the etalon pressure was adjusted to compensate for variations of etalon temperature. Then the photomultiplier counts (i.e., intensity) were adjusted to account for temporal intensity variations of the sky by dividing by the photometer reading, which was recorded in kilorayleighs. Finally, the background signal was subtracted.

C. Fourier Cosine Transform Smoothing

The Fabry-Perot interferometer produces a series of concentric rings. The center of this image is monitored by a photomultiplier tube and as the etalon pressure is changed, the measured intensity changes. A series of 34 different pressure readings were taken in each scan. The resulting observed profile is a convolution of the actual sky profile and the instrument function, with noise superimposed. To extract this noise a Fourier technique was used.

A Fourier cosine transform is fit to the data from one fringe. When the first six coefficients are used to reconstruct the curve, the result is a smoothed version of the data as shown in the equations below. If not enough coefficients are taken, the data are not accurately represented. On the other hand, if too many coefficients are taken, the resulting curve fits statistical noise as well as the source variation.

For a theoretical emission profile which is perfectly smooth, the coefficients decrease as the wavenumber (i.e., m in equation (1)) increases, as shown by Hays and Roble [1]. For our data, the coefficients decrease until m is 6, whereupon it begins to increase, as shown in Figure 4. Therefore, to represent the actual data with a curve that is as accurate as possible with minimum noise, the optimum number of coefficients is 6. Each of the three curves shown in Figure 4 are from different pressure scans, all taken successively; therefore, each curve corresponds to a different fringe.

The smoothed profiles of the observed data are given by:

$$Y = \sum_{m=1}^{6} Y_m \cos(mx), \qquad (1)$$

where the Y_m's are the Fourier coefficients from fits to the observed data. These coefficients are found using:

$$Y_m = 1/\pi \sqrt{Y_{cm}^2 + Y_{sm}^2},$$

where

$$Y_{cm} = \sum_{i=1}^{34} \frac{C}{m} \left[2 \sin(c2\, P_i) \left(\sin c2 \frac{DPS}{2}\right)^2 + \cos(c2\, P_i) \sin(c2\, DPS)\right]$$

where

$$C = \text{counts at ith step}$$

$$P_i = \text{pressure at ith step}$$

$$c2 = \frac{2\pi \times m}{SRS}$$

$$SRS = \text{free spectral range, pressure units}$$

$$DPS = P_i - P_{i-1};$$

and similarly,

$$Y_{sm} = \sum_{i=1}^{34} \frac{C}{m} \; [2 \cos (c2\, P_i) \; (\sin c2 \; \frac{DPS}{2})^2$$

$$- \sin (c2\, P_i) \sin (c2\, DPS)] \; .$$

D. Deconvolution

The smoothed profile is assumed to be a convolution of the theoretical Doppler profile of the sky emission (D) and the instrument profile (L) (obtained by observing through the instrument a diffuse illumination provided by an He-Ne laser); i.e.,

$$Y_m = D_m * L_m \; .$$

To deconvolve the laser profile from the observed data, the coefficients from the observed data were divided by the laser coefficients using the convolution theorem (e.g., see Reference 16); i.e.,

$$D_m = Y_m / L_m ,$$

where the laser coefficients are found by running a slightly modified version of the program (in Appendix D) independently for the laser fringe coefficients only.

E. Least Squares Fit

After fitting the data to a smoothed profile using the Fourier coefficients and deconvolving the instrument function, the profile is then compared to a series of theoretical Gaussian emission profiles. These theoretical profiles are discussed in Appendix A. They have a known Doppler width for any given temperature. These theoretical profiles are convolved with a Gaussian instrument function obtained by calibrating with an He-Ne laser (as in equation (2)). The theoretical curve that gives the least square error with the smoothed data was used to obtain the temperature.

To ensure that the deconvolved profiles are Gaussian, they are plotted with theoretical Gaussians as shown in Figure 5. Non-Gaussian results were not included in temperature plots. Also, the half widths of all deconvolved profiles have been compared to those in Table A-1, Appendix A to ensure that no major errors occurred in the deconvolving calculation.

V. RESULTS AND DISCUSSION

After converting the fringes to temperatures, the temperatures were plotted as a function of time for each night of observation, as shown in Figures 6a-g. Each direction of observation: zenith, north, south, east, and west (all magnetic) were included. The times given are in Universal Time (UT), where local time was 9 hours behind UT.

It is apparent from the results in Figures 6a-g that the data points are scattered, but are typically within a band that is ±100 K about the mean. The data for March 7 (Figure 6a) are highly scattered, but on March 10, the temperature is seen to be about 800±100 K. The next three nights give temperatures of 750, 750, and 800 K. All the above data were taken on clear nights. March 14 was cloudy and the apparent temperature was found to be 750 K. March 15 was foggy and the apparent temperature was found to be 700 K. On March 16, only four zenith points were taken and three of these were at about 680 K.

Contributions to the spread in the data may be from both the instrument and actual variations in OI emission intensity. It is difficult to determine the fractional contributions of these components, although it has been considered by Hays and Roble [1].

A. MSIS

Also plotted in Figures 6a-g are the temperature profiles derived from the MSIS (Mass Spectrometer Incoherent Scatter) model of the neutral atmosphere [17-18]. Parameters utilized in this model include local time, altitude, location, 3-month average $F_{10.7}$ flux, daily $F_{10.7}$ flux, and daily Ap value (see Appendix B). An example of the MSIS output is given in Appendix C.

The purpose of running MSIS was to deduce the predicted model thermospheric temperature for the geomagnetic conditions at the observing location. Comparisons of the MSIS temperatures with our results show that ours are in a reasonable range.

TABLE 1. PLOT SUMMARY

Date (UT)	MSIS Height (km)	Temp. (K)	Sky
March 7		high dispersed	clear
March 10	180	800±100	clear
March 11	170	750±100	clear
March 12	170	750±100	clear
March 13	170	800±100	clear
March 14	170	750±100	cloud
March 15	150	700±100	fog
March 16	minimal data	680	clear

B. Shadow Height

In order to determine whether the observed volumes were sunlit, the Earth's "shadow height" was calculated. Heights for zenith, north, south, east, and west (magnetic) observations were calculated. It was determined that the observed volumes in some of the observations (taken shortly after sundown and shortly before sunrise) were sunlit. Plotted in Figures 6a-g are heights of the Earth's shadow. This shadow height is the distance from the point where the line of observation intersects the surface between sunlight and shadow to the ground directly below. (See Appendix E for a detailed explanation of how shadow height is determined.)

Each curve corresponds to a given direction of observation (e.g., east). Where the curve intersects an MSIS altitude curve, the corresponding time indicates when the shadow height was at the altitude of the MSIS curve. For example, in Figure 6a, the vertical curve shown corresponds to observation toward the east. This curve intersects the MSIS 170 km curve at 1400 UT, indicating the shadow height at that time. As shown, the shadow height passed through lower altitudes at later times. The overall curve indicates sunrise, because observation points to the left of the curve are in darkness, while observation points to the right, i.e., later in time, are sunlit. In the following figures, different directions of observation are included. N represents north, while W and E represent west and east, respectively, Also shown in the figures are the curves for sunset. Of all directions observed, points to the west were the last to remain sunlit on any given night, and points to the east were the first to become sunlit.

For sunrise observations, the lowest shadow heights were to the east It can be seen that on March 11 and 13, observations to the east, an hour after the emission region passed into sunlight, indicate pre-dawn temperature enhancement. After sunset, the lowest shadow heights were to the west, but sunlit dusk observations were made only on March 14, which was a cloudy night.

Shadow height calculations were based on Chamberlain's work [19]. Figure 7 shows the resulting shadow heights as a function of time for all directions observed. Programs in Appendix E were used to obtain these results.

C. Volume Emission Rate Profiles Previously Measured

Altitude profiles of the 6300 Å volume emission rate have been reported by various investigators using data from the Atmosphere Explorer program. Selected results are noted here for comparison with the results presented in the previous section. For example, Abreau et al. [20] found altitude profiles of the volume emission rate using a photometer onboard the AE-E satellite. From November 1980 to February 1981, averaged data gave a peak rate at altitudes of 250-280 km.

Hays et al. [21] reported altitude profiles of the 6300 Å volume emission rate for various solar zenith angles during evening twilight. Peak emissions were in the 220-250 km altitude region. Their theoretical models using O_2 photodissociation and photoelectron impact indicated that below 200 km, the dominant mechanism of excitation was photodissociation.

Mid-latitude orbit data for summer and winter were examined by Torr et al. [22]. Theoretical and measured peak emission altitudes were approximately 200 km in winter and 200 km in summer.

Hernandez and Roble [10] obtained temperatures from the 6300 Å emission as a function of time. Their temperatures were found to be greater than MSIS model predictions for an altitude of 250 km during summer and equinox nights. Their data for March 1976 (the same month as our data) were scattered to about the same degree as our data, and their data were centered on 800 K in agreement with our results. Further results were later reported by Hernandez and Roble [11]. They found that the 6300 Å line peak emission rate occurred below the F_2 peak at 250 km, at about 100 R, decreasing throughout the night.

Recently, Sipler et al. [23] also measured the neutral F-region temperature using a Fabry-Perot interferometer. During geomagnetically quiet nights from 1975 to 1979, equinox solar minimum average temperatures were found to be about 750 K.

Emission rate profiles for 6300 dayglow were reported by Killeen et al. [24]. They reported that a typical profile had a peak of 180 cm^{-3} s^{-1} at about 210 km altitude.

The above results indicate a peak volume emission rate at altitudes of 200-300 km. As discussed earlier, these results are in rough agreement with the present observations, given the spread in our temperatures and the combined uncertainties of MSIS temperatures, as well as our lack of statistical data. Assuming the glow intensity is originating from 200 km, our data suggest the MSIS model is predicting slightly higher temperatures than observed.

VI. FUTURE WORK

Many improvements could be made to the apparatus. With CCD arrays now readily available, it is possible to image the Fabry-Perot fringes. Imaging of fringes has been done by Sivjee et al. [15] and Rees and Greenaway [25]. The latter investigators developed a Doppler imaging system (DIS) which used a Fabry-Perot interferometer and a 120° field of view all-sky camera. The multiring image contains spectral and spatial information. By imaging the fringe from the interferometer (of this investigation), all the information could be digitized and analyzed by computer. By using the entire image of the fringe rather than just the central fringe, a much stronger signal is obtained. This system would provide a convenient means of monitoring winds using the Doppler shift. Yet another advantage of this system would be that fringes would be made much more quickly than with pressure scanning. Further, integration times could be easily varied to an optimum duration. This system could be further enhanced by using a pyramid with mirror surfaces rather than a scanning mirror. This would allow monitoring of all four directions simultaneously. With both of the above modifications, all moving parts would be eliminated, greatly simplifying the entire system and reducing its size.

An extension of the pyramid system would be to use an all-sky lens so that all directions could be monitored simultaneously. This lens could be coupled to an interference filter, an image intensifier, and finally to a CCD array via a fiber optic plug. In this arrangement, the apparatus could be considerably reduced in size compared with the current system. However, as size decreases, integration time increases. An image intensifier could be used to reduce integration time.

Cooling of the array would be imperative to reduce noise accumulation. A Peltier electric cooler, for example, would be convenient for this task.

VII. CONCLUSION

The temperatures of the 6300 line on the clear nights of March 10, 11, 12, and 13 were 800, 750, 750, and 800 K, respectively, with a spread of

±100 K. Despite the large spread in the data, the temperatures and the spread in the temperatures were consistent from day to day, and consistent with previous observations.

REFERENCES

1. Hays, P. B. and Roble, R. G.: A Technique for Recovering Doppler Line Profiles from Fabry-Perot Interferometer Fringes of Very Low Intensity. Applied Optics, Vol. 10, 1971, p. 193.

2. Roble, R. G.: A Theoretical and Experimental Study of the Stable Mid-Latitude Red Arc (SAR-ARC). Ph.D. Thesis, University of Michigan, 1969.

3. Wark, D. Q.: Doppler Widths of the Atomic Oxygen Lines in the Airglow. Astrophys. J., Vol. 131, 1960, p. 491.

4. Nilson, J. A. and Shepherd, G. G.: Upper Atmospheric Temperatures from Doppler Line Widths--I. Some Preliminary Measurements on OI 5577 Å in Aurora. Planet. Space Sci., Vol. 5, 1961, p. 299.

5. Turgeon, E. C. and Shepherd, G. G.: Upper Atmospheric Temperatures from Doppler Line Widths--II. Measurements on the OI 5577 and OI 6300 Å Lines in Aurora. Planet Space. Sci., Vol. 9, 1962, p. 295.

6. Zwick, H. H. and Shepherd, G. G.: Upper Atmospheric Temperatures from Doppler Line Widths--V. Auroral Electron Energy Spectra and Fluxes Deduced from the 5577 and 6300 Å Atomic Oxygen Emissions. Planet. Space Sci., Vol. 21, 1973, p. 605.

7. Hernandez, G.: Measurement of Thermospheric Temperatures and Winds by Remote Fabry-Perot Spectrometry. Opt. Eng., Vol. 19, 1980, p. 518.

8. Hernandez, G. and Roble, R. G.: Direct Measurements of Nighttime Thermospheric Winds and Temperatures. 1. Seasonal Variations During Geomagnetic Quiet Period. J. Geophys. Res., Vol. 81, 1976, p. 2065.

9. Hernandez, G. and Roble, R. G.: Direct Measurements of Nighttime Thermospheric Winds and Temperatures. 2. Geomagnetic Storms. J. Geophys. Res., Vol. 81, 1976, p. 5173.

10. Hernandez, G. and Roble, R. G.: Direct Measurements of Nighttime Thermospheric Winds and Temperatures. 3. Monthly Variations During Solar Minimum. J. Geophys. Res., Vol. 82, 1977, p. 5505.

11. Hernandez, G. and Roble, R. G.: Thermospheric Dynamics Investigations with Very High Resolution Spectrometers. Applied Optics, Vol. 18, 1979, p. 3376.

12. Smith, R. W., Sivjee, G. G., Stewart, R. D., McCormac, F. G., and Deehr, C. S.: Polar Cusp Ion Drift Studies Through High-Resolution Interferometry of O^+ 7320-Å Emission. J. Geophys. Res., Vol. 87, 1982, p. 4455.

13. Born, M. and Wolf, E.: Principles of Optics. McMillan Co., New York, 1964.

14. Hernandez, G.: Analytical Description of a Fabry-Perot Spectrometer. Applied Optics, Vol. 5, 1966, p. 1745.

15. Sivjee, G. G., Hallinan, T. J., and Swenson, G. R.: Fabry-Perot-Interferometer Imaging System for Thermospheric Temperature and Wind Measurements. Applied Optics, Vol. 19, 1980, p. 2206.

16. Bracewell, R.: The Fourier Transform and Its Applications. McGraw-Hill, New York, 1965.

17. Hedin, A. E., Mayr, H. G., Reber, C. A., Spencer, N. W., and Carignan, G. R.: Empirical Model of Global Thermospheric Temperature and Composition Based on Data from the Ogo 6 Quadrupole Mass Spectrometer. J. Geophys. Res., Vol. 79, 1974, p. 215.

18. Mayr, H. G., Harris, I., Hedin, A. E., Spencer, N. W., and Wharton, L. E.: Thermospheric Superrotation Revisited. J. Geophys. Res., Vol. 89, 1984, p. 5613.

19. Chamberlain, J. W.: Physics of the Aurora and Airglow. Academic Press, New York, 1961.

20. Abreau, V. J., Schmitt, G. A., Hays, P. B., and Dachev, T. P.: Volume Emission Rate Profiles of the 6300-Å Tropical Nightglow Obtained from the AE-E Satellite: Latitudinal and Seasonal Variations. J. Geophys. Res., Vol. 87, 1982, p. 6346.

21. Hays, P. B., Rusch, D. W., Roble, R. G., and Walker, J.C.G.: The OI (6300 Å) Airglow. Rev. Geophys. Space Phys., Vol. 16, 1978, p. 225.

22. Torr, D. G., Richards, P. G., Torr, M. R., and Abreau, V. J.: Further Quantification of the Sources and Sinks of Thermospheric $O^1(D)$ Atoms. Planet. Space Sci., Vol. 29, 1981, p. 595.

23. Sipler, D. P., Luokkala, B. B., and Biondi, M. A.: Fabry-Perot Determinations of Midlatitude F-Region Neutral Winds and Temperatures from 1975 to 1979. Planet. Space Sci., Vol. 20, 1982, p. 1025.

24. Killeen, T. L., Hays, P. B., Spencer, N. W., and Wharton, L. E.: Neutral Winds in the Polar Thermosphere as Measured from Dynamics Explorer. Geophys. Res. Lett., Vol. 9, 1982, p. 957.

25. Rees, D. and Greenaway, A. H.: Doppler Imaging System; an Optical Device for Measuring Vector Winds. 1: General Principles. Applied Optics, Vol. 22, 1983, p. 1078.

26. Griem, H. R.: Plasma Spectroscopy. McGraw Hill, New York, 1964.

ORIGINAL PAGE IS
OF POOR QUALITY

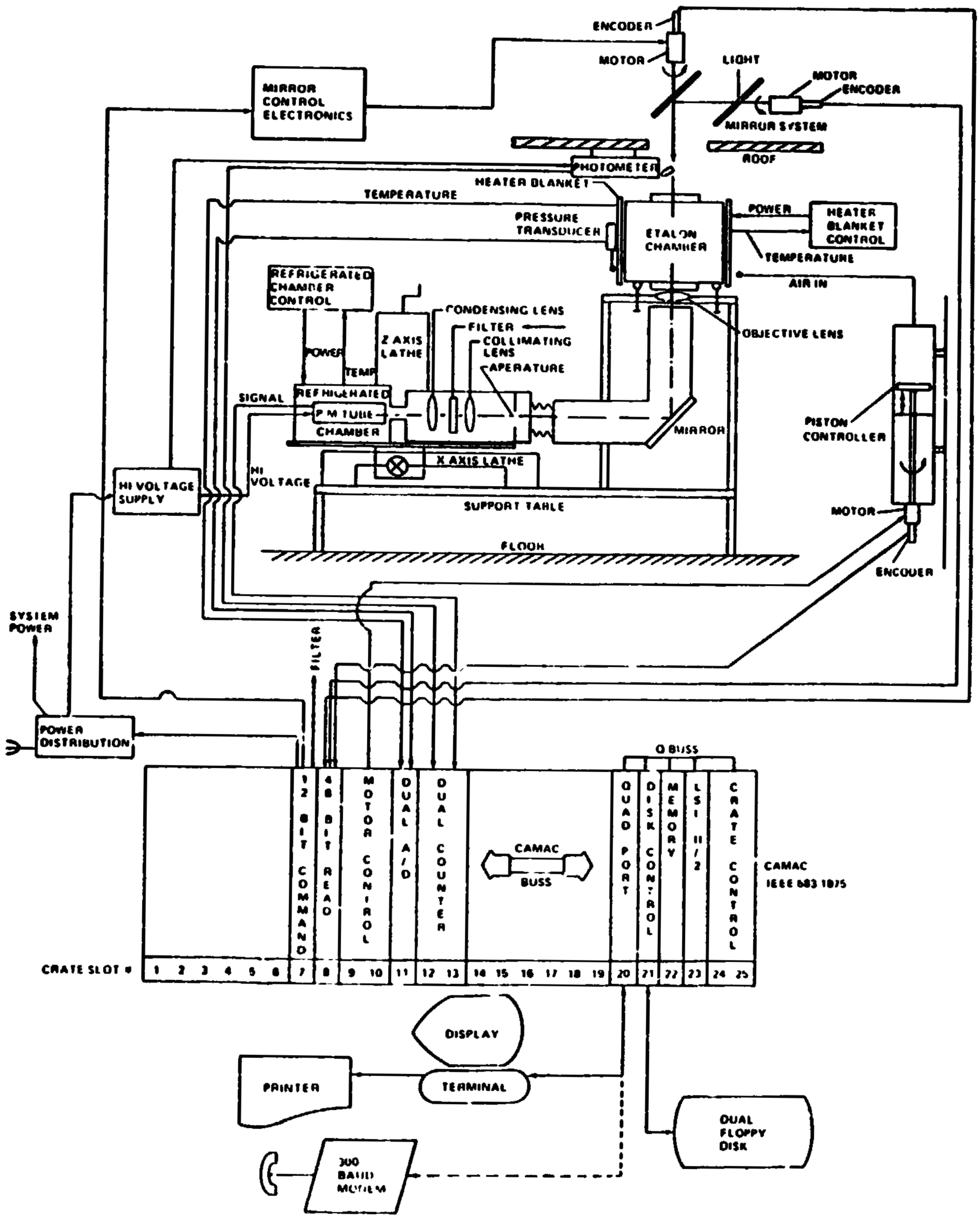

Figure 1. Fabry-Perot Interferometer control schematic.

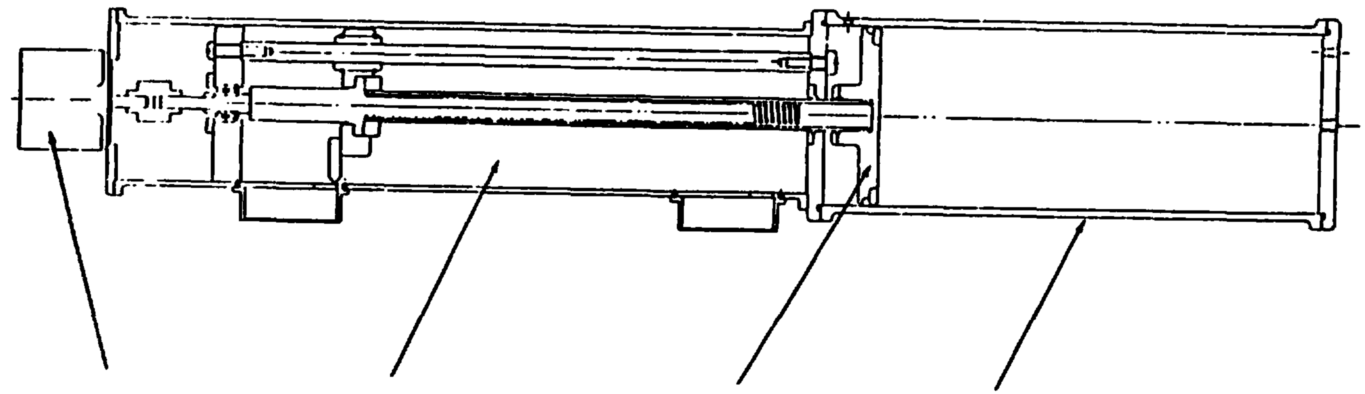

Figure 2. Fabry-Perot Interferometer piston diagram.

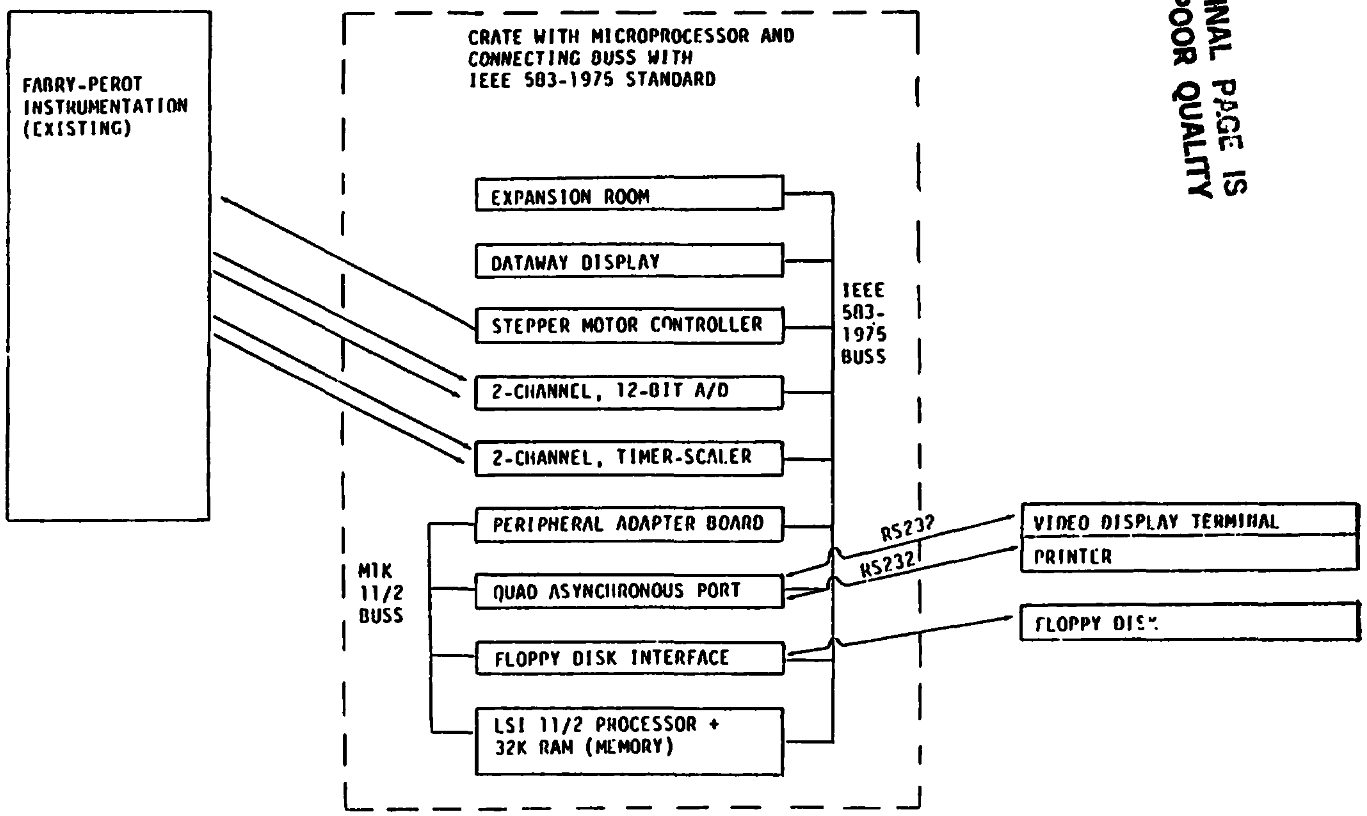

Figure 3. Fabry-Perot Interferometer controller and data acquisition and display system schematic.

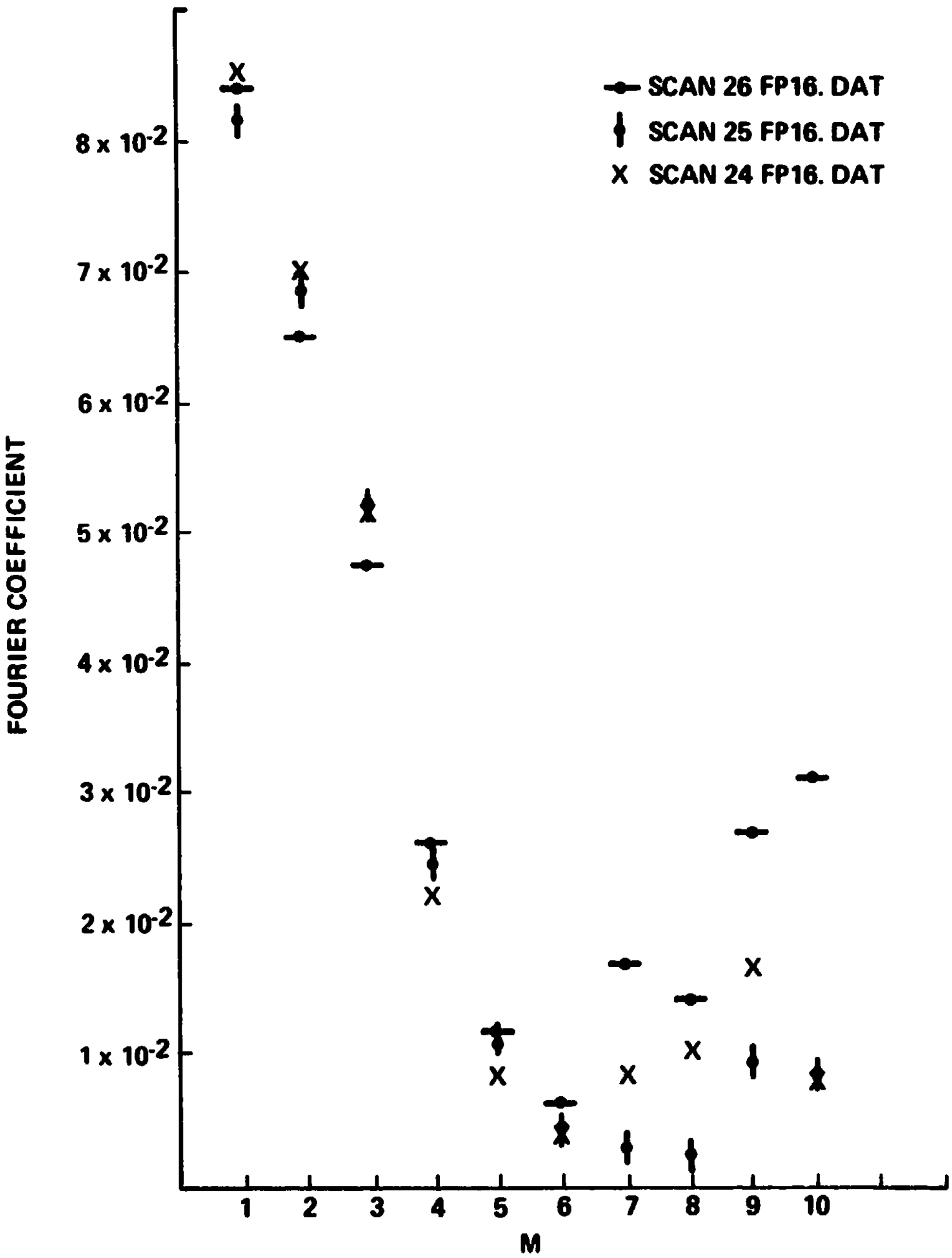

Figure 4. Optimization of number of Fourier coefficients.

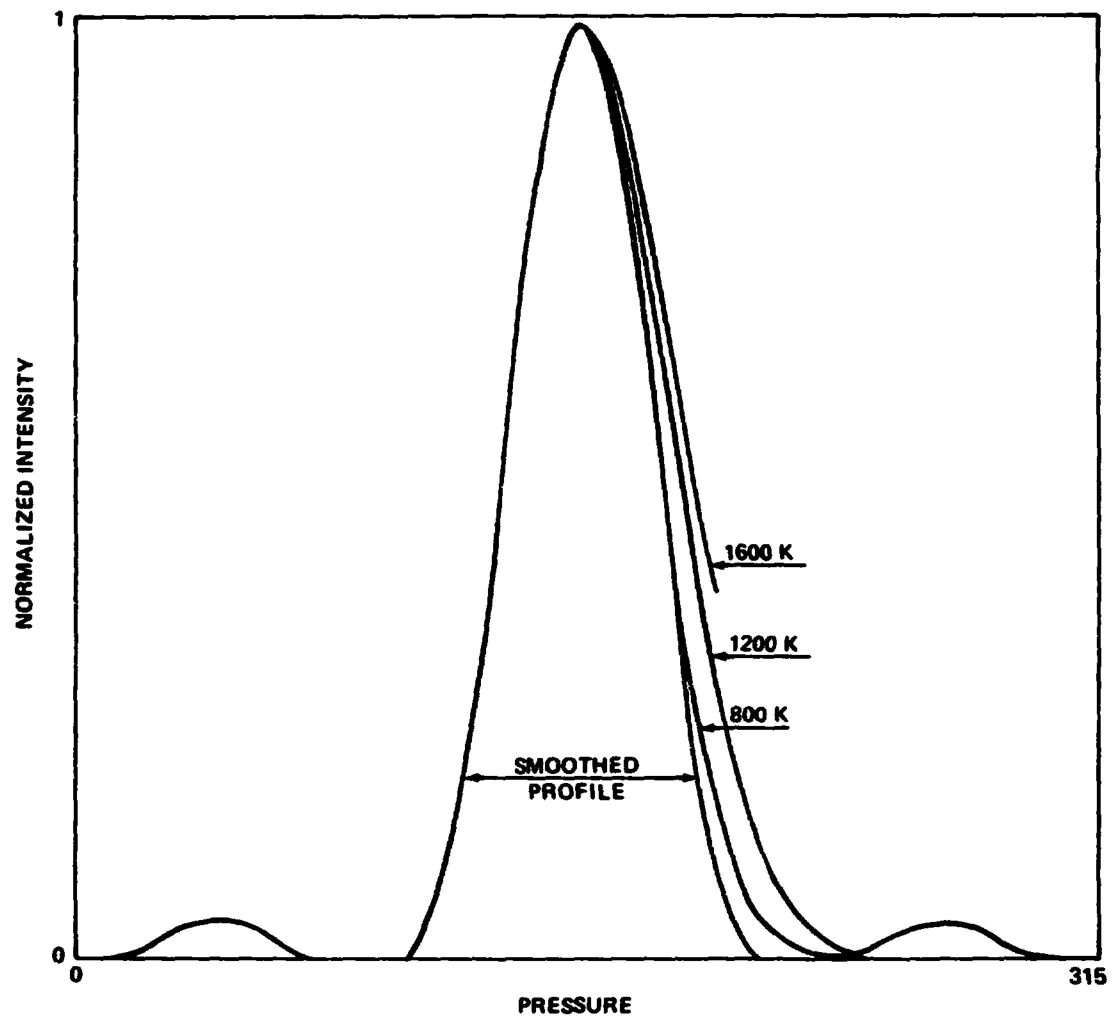

Figure 5. Comparison of theoretical Gaussian profiles to smoothed data.

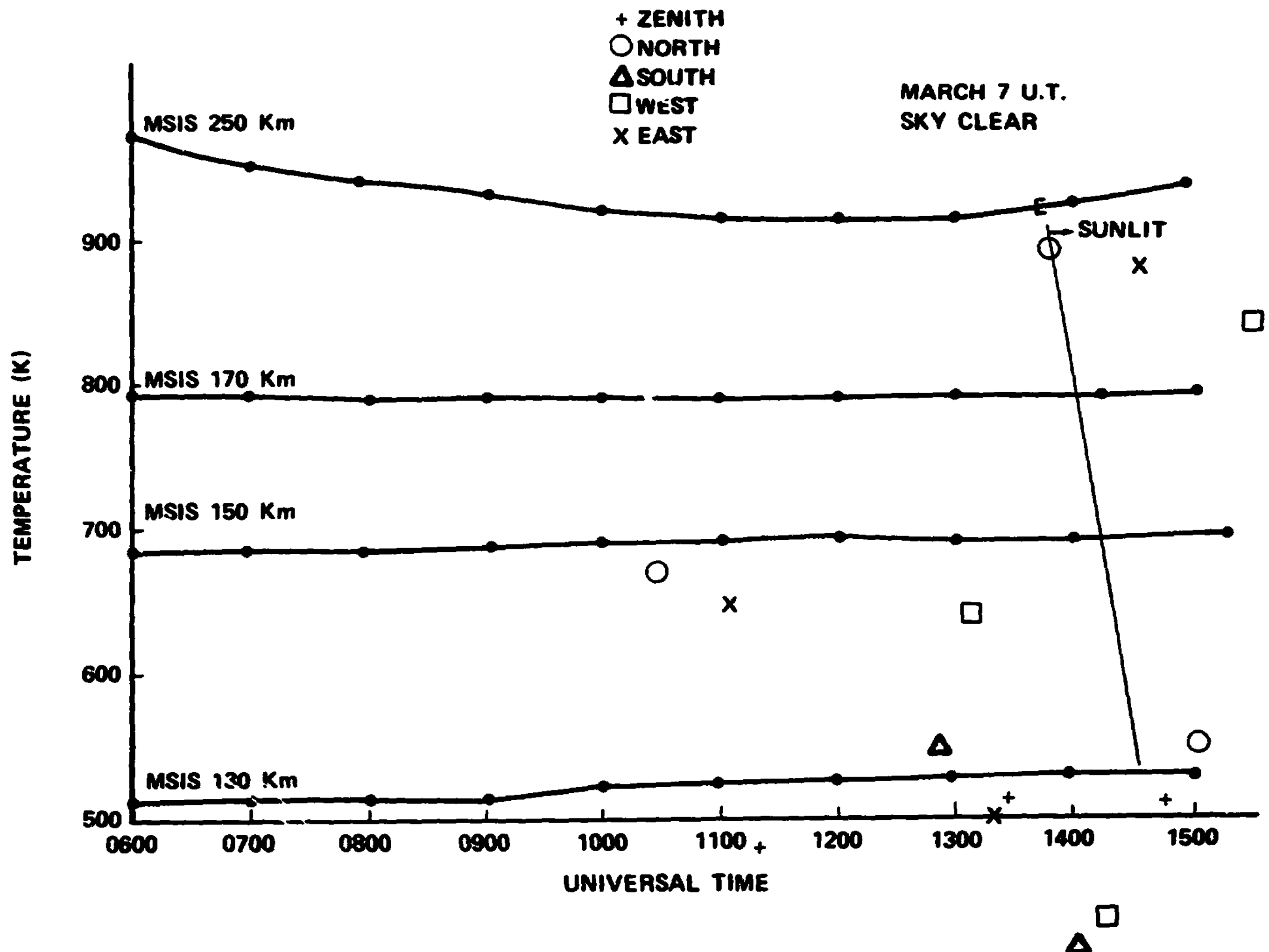

(a)

Figure 6. Comparisons of observed temperatures with MSIS temperatures, plotted versus Universal Time. (a) March 7, 1984, (b), March 10, (c) March 11, (d) March 12, (e) March 13, (f) March 14, (g) March 15.

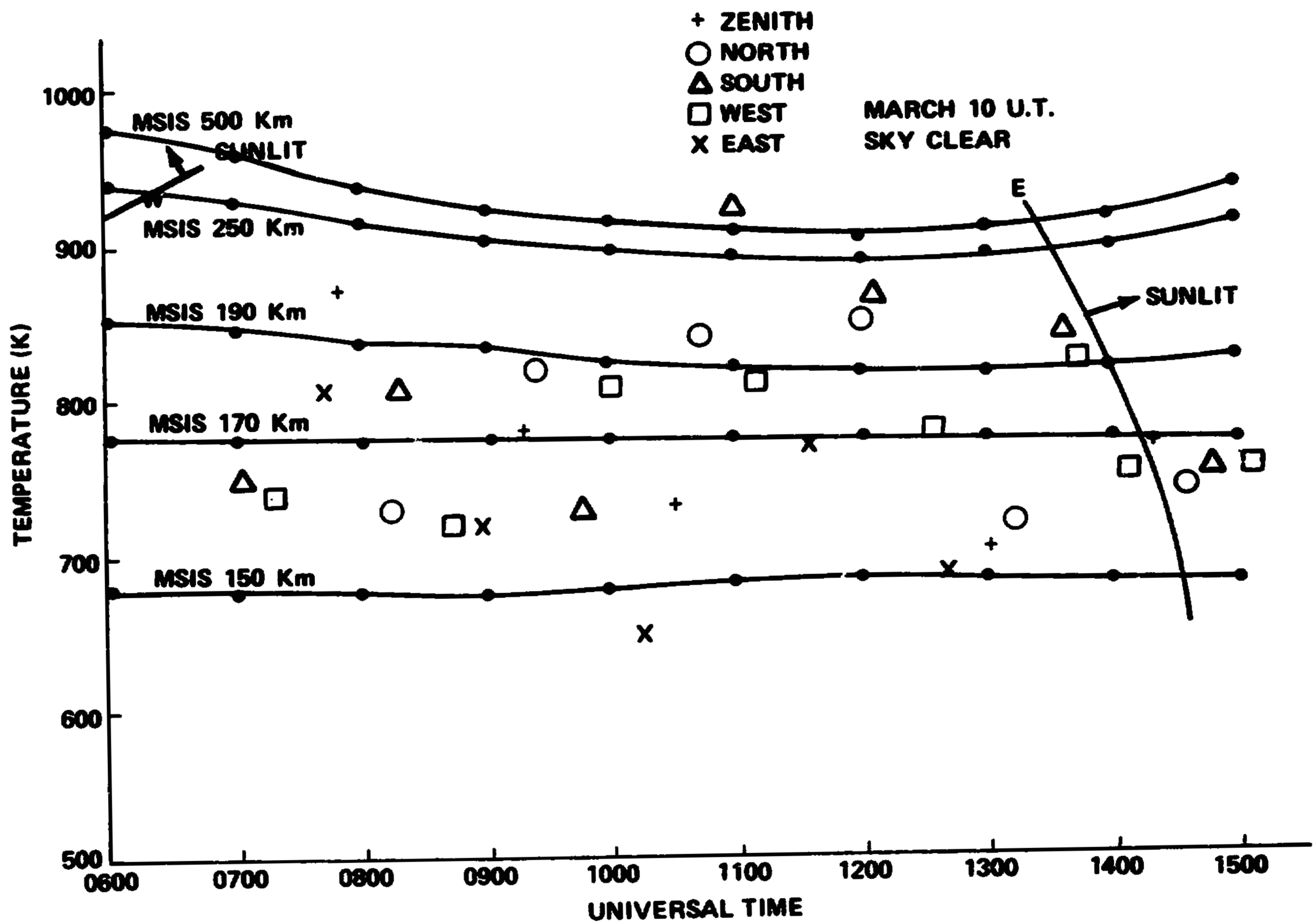

Figure 6b. March 10

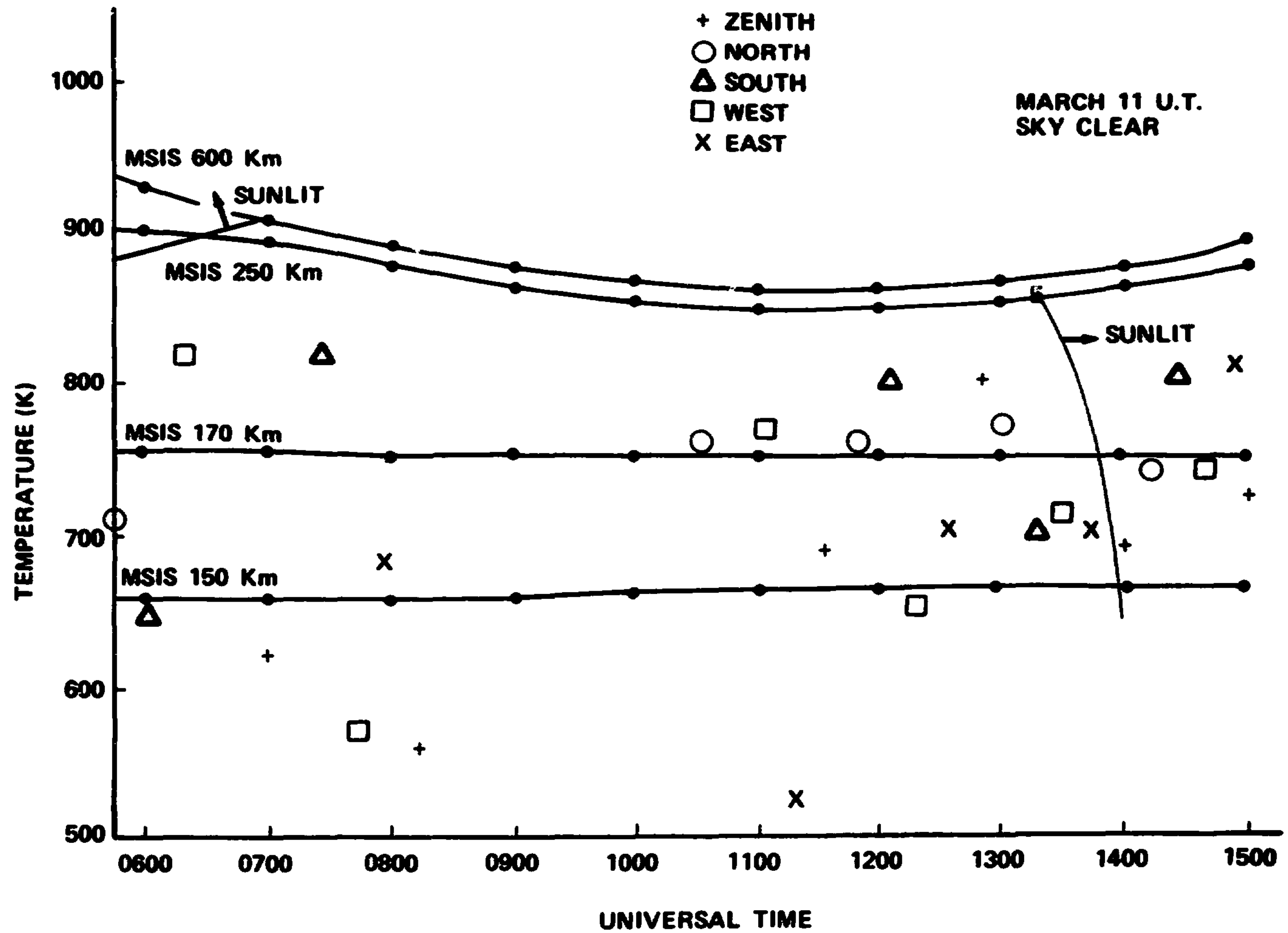

Figure 6c. March 11.

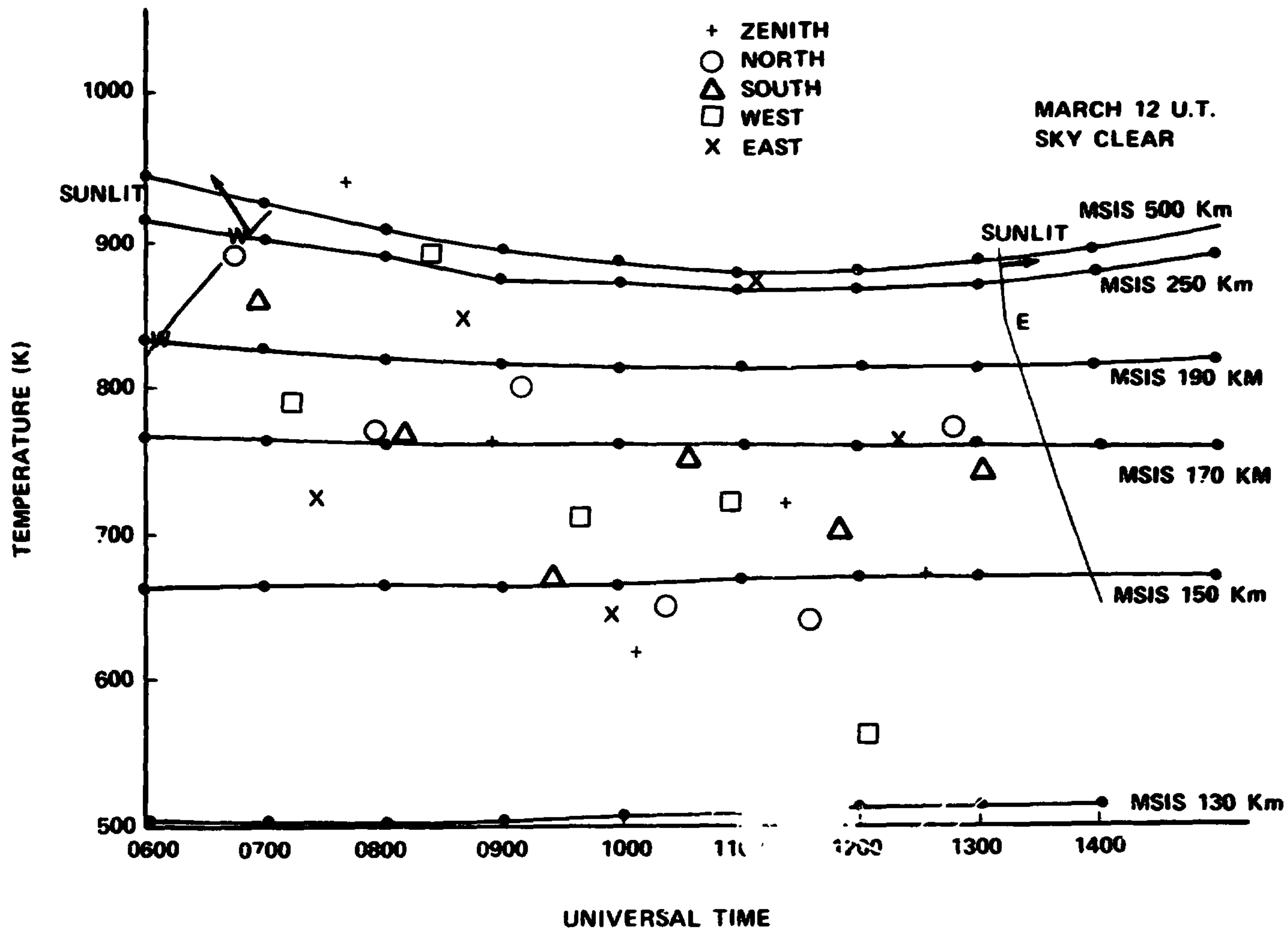

Figure 6d. March 12.

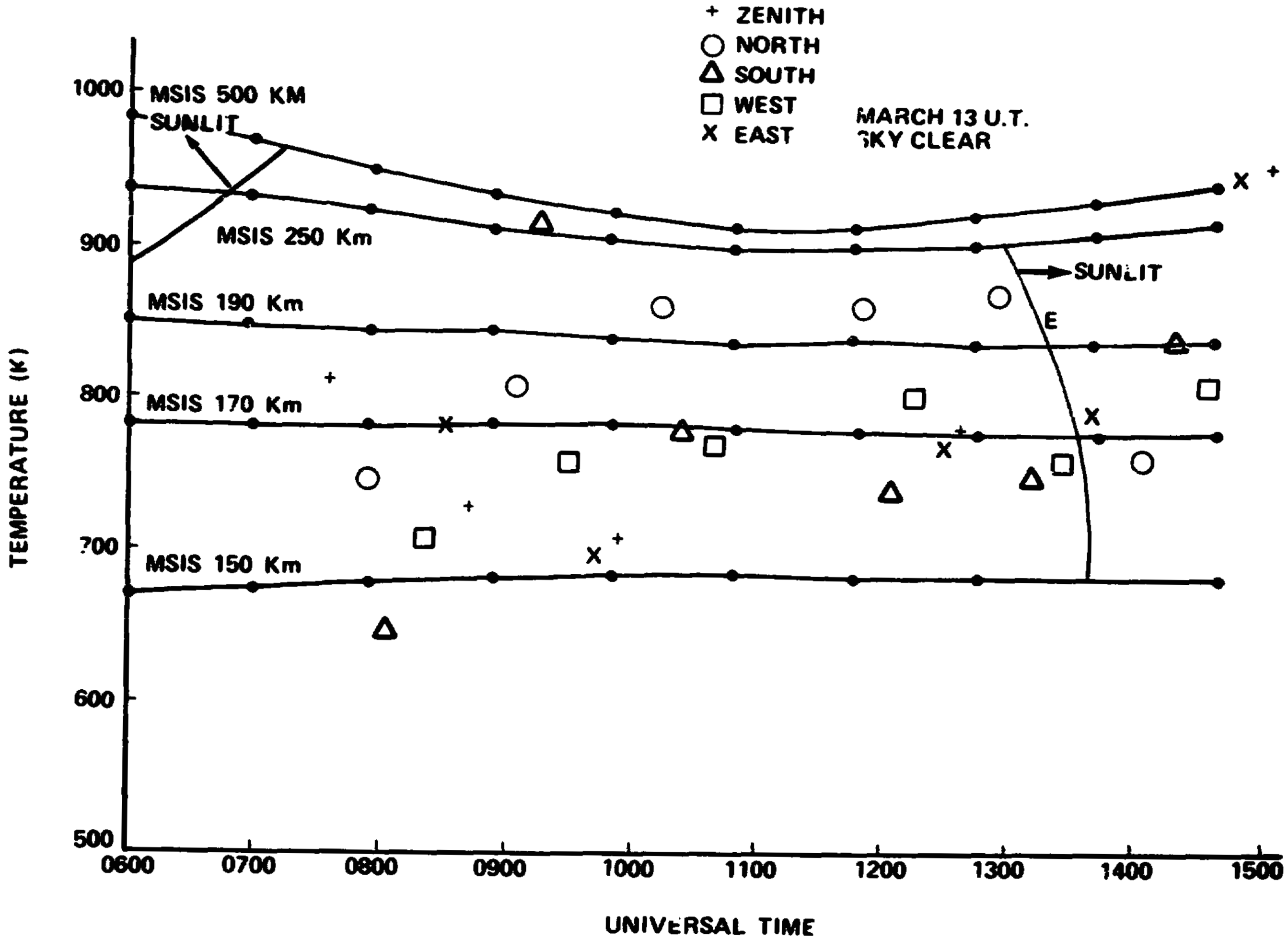

Figure 6e. March 13.

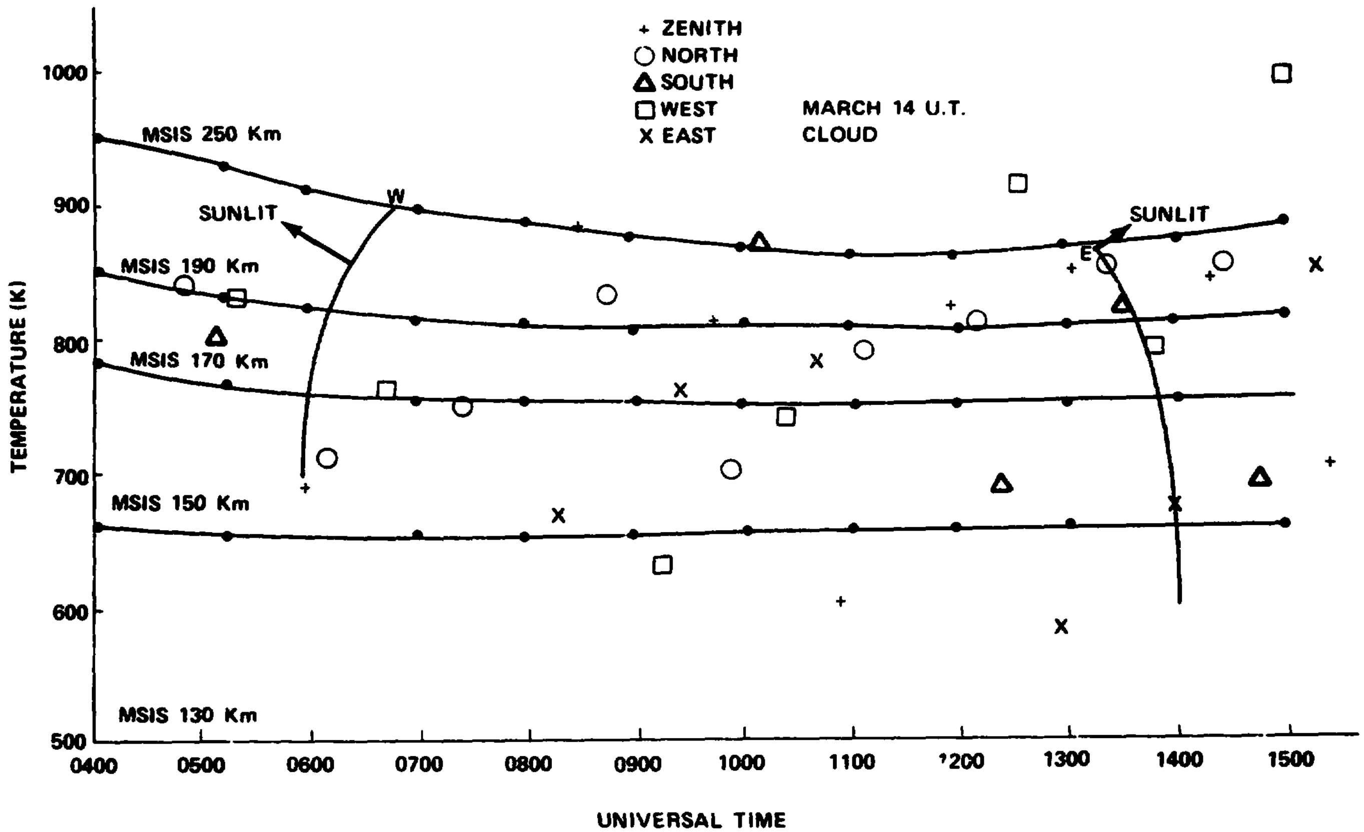

Figure 6f. March 14.

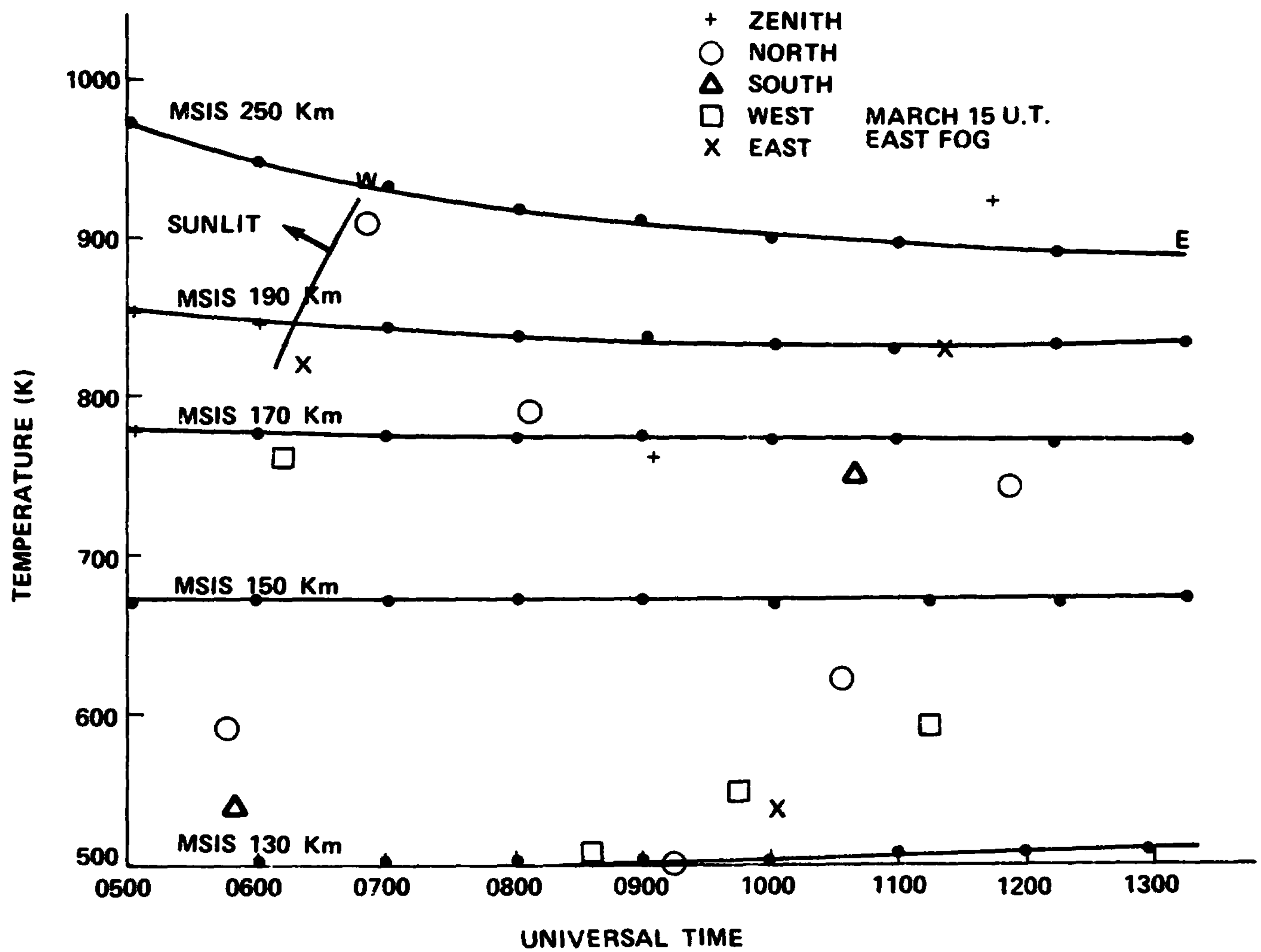

Figure 6g. March 15.

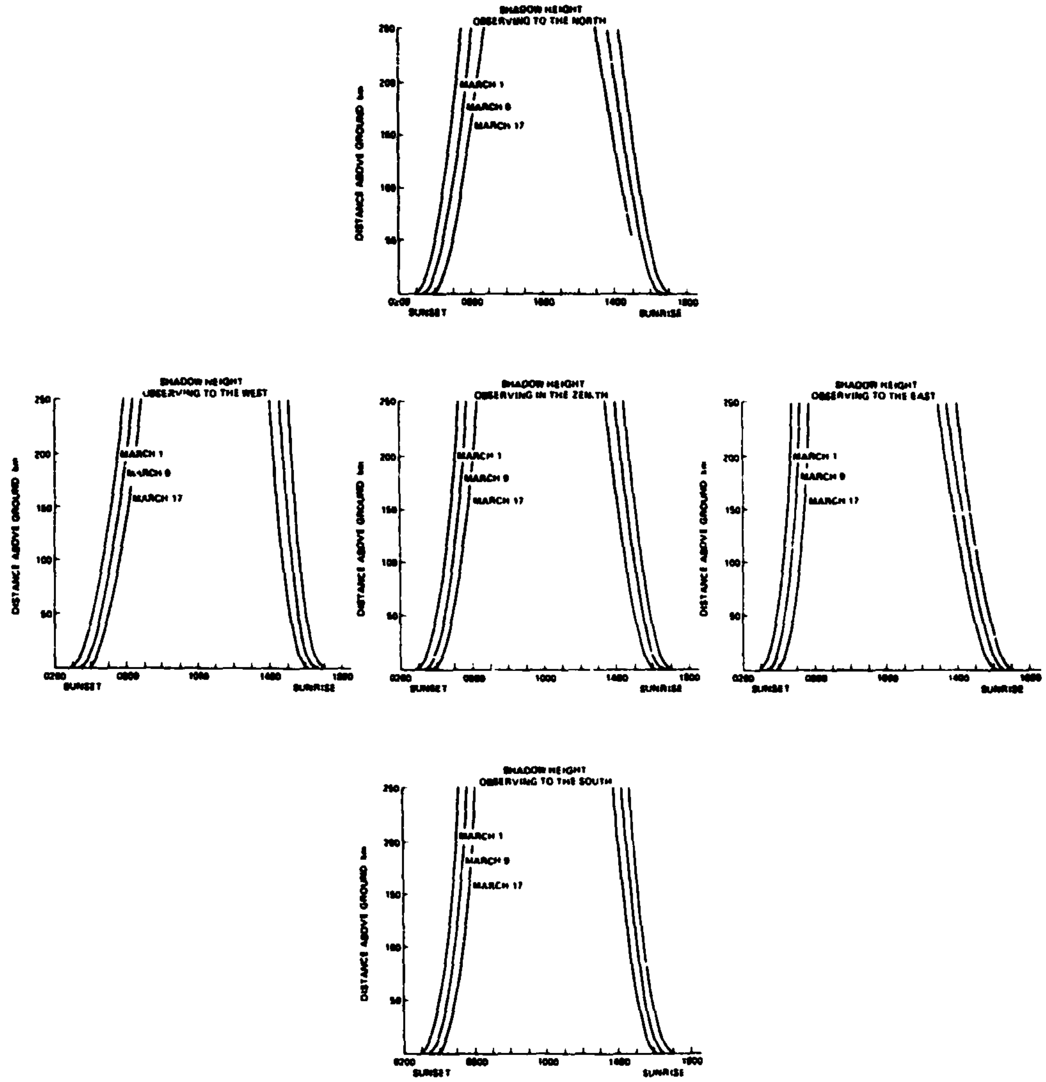

Figure 7. Shadow height as a function of Local Time in different look directions for days encompassing the period of the observations.

APPENDIX A. THEORETICAL GAUSSIAN PROFILES

A Doppler shift of wavelength results from the motion of a radiating particle towards or away from an observer. In gas or plasmas, the random thermal motions of all particles lead to a Maxwellian velocity distribution. This results in a Gaussian distribution in observed frequency due to the Doppler shifting. Hence, the spectral profile has a Doppler broadened component that is a function of temperature. From Griem [26], the Doppler shape is given by

$$I(\Delta\lambda) = \left\{\frac{Mc^2}{2\pi kt\lambda_o^2}\right\}^{\frac{1}{2}} \exp\left\{\frac{-Mc^2}{2ky\lambda_o^2}(\Delta\lambda)^2\right\}, \qquad \text{(A-1)}$$

where λ_o = 6300 Å = 6.3×10^{-7} m, c = 2.99792×10^8 m/s, M = mass of emitting species (0) (= 2.6776×10^{-26} kg), k = Boltzman's constant (= 1.38×10^{-23} J/K), and T = temperature in K.

Normalized intensity as a function of T and $\Delta\lambda$ is found from:

$$\text{Normalized Intensity} = \exp\left\{-2.19682568 \times 10^{26} \frac{(\Delta\lambda)^2}{T}\right\} .$$

The above equation is verified as shown in Appendix G, by comparing it with Wark's [3] version of this equation.

Theoretical Gaussian Profiles

To convert the form of this equation to one in terms of etalon pressure instead of wavelength, λ, the conversion

$$\Delta\lambda = \frac{1.98 \times 10^{-11} \text{ mFSR}}{74.09 \text{ pressure units FSR}} \times \Delta \text{ pressure units} \qquad \text{(A-2)}$$

is substituted into equation (A-1) to obtain:

$$\text{Normalized Intensity} = \exp\left\{-15.689416 \ \frac{(\Delta \text{ pressure units})^2}{T}\right\},$$

where FSR is Free Spectral Range and T is temperature in K.

The factor (1.98×10^{-11} m FSR) is a fixed instrument parameter. The FSR observed with the calibration was 75.53 pressure units, and this value is used throughout the program and in the calculations except in the above step. Here, a slightly smaller FSR was used to compensate for the fact that the 6328 Å laser was used for calibration, while the observations were of 6300 Å. Since the FSR is proportional to the square of the incident wavelength, the 6328 He-Ne laser which gave a FSR of 75.53 would, at 6300 Å, have given an FSR of:

$$75.53 \left(\frac{6300}{6328}\right)^2 = 74.86$$

So the FSR of 75.53 was 75.53 - 74.86 = 0.67 pressure units too high. To compensate for this, the FSR used in the above step (equation (A-2)) is approximately 75 pressure units.

To input Δ pressure units in radians x 100 (where 2π rad of transformed data corresponds to 1 FSR of data), the conversion for each set of data

$$\frac{75.53 \text{ pressure units}}{2\pi \text{ rad} \times 100} = \frac{12.02097}{100} \qquad \text{(A-3)}$$

is substituted into equation (A-2) to obtain:

$$\text{Normalized Intensity} = \exp\left\{0.2267 \ \frac{(\Delta \text{ rad})^2}{T}\right\},$$

where the numerical factor 0.2267 is labeled "CO" in the program. The reason for scaling the pressure units by the factor 100 is to make a unit change in input (equation (A-3)) small enough to allow many ($628 \sim 100 \times 2 \times \pi$) steps per fringe. This facilitated programming of the graphics.

To check the results of the program, the HWHMs of the laser and theoretical Gaussians can be easily convolved. The laser width of 3.5 pressure units was obtained from a pressure and temperature compensated laser calibration scan. To find the HWHM of the theoretical Gaussians start with equation (A-2).

$$\text{Normalized Intensity} = \exp\left\{-15.689\,\frac{(\text{pressure units})^2}{T}\right\}.$$

Let normalized intensity = 0.5 (i.e., HWHM), then solve for pressure units to obtain:

$$\text{HWHM in pressure units} = \sqrt{\frac{T\ \ln 0.5}{-15.689}}\ .$$

Convolving this with the laser calibration scan width provides a quick look determination of the temperature from the observed width. Examples are shown in Table A-1.

TABLE A-1. QUICK-LOOK DETERMINATION OF TEMPERATURE FROM OBSERVED WIDTH

Temperature (K)	Theoretical Gaussian HWHM (pressure units=psi)	Convolution of Theoretical Gaussian and Laser $\sqrt{HWHM^2 + 3.5^2}$ (pressure units=psi)
1000	6.646	7.51
1100	6.97	7.80
1200	7.28	8.078
1300	7.57	8.3477
1400	7.86	8.608
1500	8.14	8.8611
1600	8.407	9.107
1700	8.666	9.346
1800	8.917	9.5799
1900	9.162	9.8077
2000	9.400	10.030

APPENDIX B. SOLAR GEOPHYSICAL DATA

The following data were used in the MSIS program and were obtained from NOAA [27]:

March 1984	6	7	8	9	10	11	12	13	14	15	16
Daily Average Indices Ap	31	26	29	13	17	9	11	19	6	9	16
Daily Solar Flux at 2800 MHz (10.7 cm)	109.5	105.0	103.8	102.4	98.8	98.6	102.3*	114.7	121.1	134.4	124

*Adjusted for burst in progress at time of measurement.

Mean $F_{10.7}$ for December 1983, January 1984, February 1984, and March 1984 was 90.5, 112.4, 137.2, and 120.8, respectively.

APPENDIX C. MSIS EXAMPLE OUTPUT

MARCH 7 UT

84067
INPUT UNIVERSAL TIME IN SEC
14440 (0400 UT)
INPUT MIN, MAX ALTITUDES AND ALT. STEP IN KM
130,290 20
INPUT GEODETIC LAT., EAST LONG. IN DEG
64.9,212.2
INPUT LOCAL APPARENT SOLAR TIME IN HRS
18.2
INPUT 3-MO. AVE. OF $F_{10.7}$ FLUX
112
INPUT DAILY $F_{10.7}$ FLUX FROM PREVIOUS DAY
109.5
INPUT DAILY AP VALUE
26

DATE	UT(SEC)	LATITUDE	LONGITUDE	LOCAL TIME	$\langle F_{10.7} \rangle$	$F_{10.7}$	AP
84067	14440	64.9	212.2	18.2	112.0	109.5	26

ALT	[HE]	[O]	[N2]	[O2]	[AR]	[H]	T
130.	1.7502E+07	3.2964E+10	1.1277E+11	2.0486E+10	4.8818E+08	1.4128E+06	524.
150.	1.2866E+07	1.3711E+10	3.0166E+10	4.7443E.09	8.6045E+07	5.0339E+05	692.
170.	1.0393E+07	7.1768E+09	1.1209E+10	1.5684E+09	2.2538E+07	2.5966E+05	806.
190.	8.8380E+06	4.2385E+09	4.8880E+09	6.1621E+08	7.1885E+06	1.7916E+05	883.
210.	7.7383E+06	2.6843E+09	2.3331E+09	2.6699E+08	2.5662E+06	1.4700E+05	936.
230.	6.8957E+06	1.7755E+09	1.1773E+09	1.2287E+08	9.8243E+05	1 3188E+05	972.
250.	6.2138E+06	1.2081E+09	6.1598E+08	5.8823E+07	3.9375E+05	1.2358E+05	996.
270.	5.6406E+06	8.3788E+08	3.3030E+08	2.8927E+07	1.6285E+05	1.1829E+05	1013.
290.	5.1460E+06	5.8885E+08	1.8022E+08	1.4498E+07	6.8877E+04	1.1441E+05	1025.

APPENDIX D. PROGRAM AND EXAMPLE OUTPUT

```
.TYPE G.G

C      PROG TO GENERATE THEORETICAL GAUSSIAN PROFILES
C      AND PLOT OBSERVED PROFILES AND FIND TEMPERATURE
C      Following is the starting point (sp) value used to
C      establish the place in the data to start reading.
       SP=1668.
C      Following is a table that appears in the report, and is not essential
C      to this program.  It is included here for reference only.
C      GENERATE A TABLE TO FIND APPROX TEMP FROM HWHM OF RAW DATA
CC     TE=700.
CC     WRITE(5,*)'******'
C      X IS TEMP, XX IS HWHM PSI, XXX IS HWHM CONVOLUTED WITH 3.5 PSI LASER
CC     WRITE(5,*)'TEMP,    HWHM THEORETICAL             HWHM CONVOLUTED '
C3     X=((TE*(ALOG(.5)))/-15.689)**.5
C      XX=X*315./27.67
C      XXX=((X*X)+(3.5*3.5))**.5
C      WRITE(5,*)TE,X,XX,XXX
C      TE=TE+100.
C      IF (TE .LE. 1700) GO TO 3
C      ************************************************************************
C      The program starts here. YSM, YSSM, and YSCM are the fourier cofficients
       DIMENSION YSM(15),YSCM(15),YSSM(15)
       REAL F(10)
C      The following step is required for graphing only and is not essential
       CALL INITT(30)
C      RETREIVE OBSERVED DATA
C      RETREIVE OBSERVED TEMP(TL), PRESSURE(PL), COUNTS(CL),
C         KILORAYLEIGHS(KL),    NP IS NEW PRESSURE, NC IS NEW # OF COUNTS
       REAL TL(34)
       REAL PL(34)
       REAL CL(34)
       REAL KL(34)
       REAL NP(34)
       REAL NC(34)
       OPEN(UNIT=3,NAME='FW2:FP16.DAT',READONLY,TYPE='OLD')
C      READ: TEMP PRES COUNTS KRAYS
C      READ BLANKS UNTIL START OF DESIRED DATA**********************
       ZW=1
       WRITE(5,*)'ZW  ZS'
 187   READ(3,*,ERR=187)
C      WRITE(5,*)ZW,ZS
       ZW=ZW+1
C      MAX ZW VALUE (SP) BELOW DETERMINES STARTING PT TO READ DATA
C      For convenience, the following step was moved to near begining of prog.
C      SP=1185.
       IF (ZW .LE. SP) GO TO 187
       ZY=1
       ZY=ZY+1
C      C      ************************************************************
```

```
C     Blanks have now been read to beginning of data.  Start reading data now.
      ZZ=1
189   READ(3,150)TL(ZZ),PL(ZZ),CL(ZZ),KL(ZZ)
C     PRESSURE AND INTENSITY COMPENSATION *********
      NP(ZZ)=PL(ZZ)*(298./(273.+TL(ZZ)))
      NC(ZZ)=CL(ZZ)/KL(ZZ)
C     ********************************************
      ZZ=ZZ+1
C     The following step tells computer to read 34 lines of data (the fringe).
      IF (ZZ .LE. 34) GO TO 189
 150  FORMAT (9X,F6.3,F7.2,15X,F6.0,4X,F5.3)
C     CALCULATE BACKGROUND INTENSITY ZB=AVERAGE OF 1ST AND LAST PTS
C       OF NC AFTER COMPENSATIONS, BEFORE SUBTRACTION OF BG AND NORMALIZATION
      ZB=(NC(1)+NC(34))/2
      WRITE(5,*)'↑↑↑↑↑↑↑↑↑↑↑↑'
      WRITE(5,*)'BACKGROUND INTENSITY IS'
      WRITE(5,*)ZB
C     Following step not required, so ignore.
C     WRITE(5,*)'NP(34)-NP(1)='
C     Following is specification of free spectral range in pressure units
      SRS=75.53
      WRITE(5,*)SRS
C     NORMALIZE NUMBER OF COUNTS AND SUBTRACT BACKGROUND
C     NORMALIZE BY DIVIDING BY 11TH ELEMENT OF NC (18TH FOR 34ELEMENTS ASBELOW)
      WRITE(5,*) 'NC BEFORE NORMALIZING AND AFTER SUBTRACTION OF BG'
      ZA=1
 149  WRITE(5,*) NC(ZA)-ZB
      ZA=ZA+1
      IF (ZA .LE. 34) GO TO 149
C     NORMALIZE TO NN=NC(11)-ZB=MIDDLE NO. OF COUNTS - Z BACKGROUND
      WX=NC(18)-ZB
      WRITE(5,*)'WX IS'
      WRITE(5,*)WX
C     The next 4 steps are used as checks only and may be ignored.
C     NN=NC(18)-ZB
C     NN=WX
CC    WRITE(5,*)'WX IS'
CC    WRITE(5,*)WX
C     The next 4 lines are the normalization described 15 lines above
      ZW=1
 152  NC(ZW)=(NC(ZW)-ZB)/WX
      ZW=ZW+1
      IF (ZW .LE. 34) GO TO 152
      WRITE(5,*)'PRESSURE, COUNTS, KILORAYLEIGHS, IN RAW DATA FORM'
      WRITE(5,*)'LAST 2 COLUMNS ARE NEW PRESSURE AND NEW COUNTS'
      WRITE(5,*)'     PL              CL              KL              NP NC'
      ZA=1
 151  WRITE(5,*)PL(ZA),CL(ZA),KL(ZA),NP(ZA),NC(ZA)
      ZA=ZA+1
      IF (ZA .LE. 34) GO TO 151
      WRITE(5,*)'THIS TEXT CAUSES LAST LINE TO PRINT'
C     100+++++++++++++++++++++++++++++++++++++++++++++++++++++++++++++++++++++
```

```
C       Next two lines are free spectral range in pressure units
        WRITE(5,*)'SRS'
        WRITE(5,*)SRS
C       Next line applies only to graphing on terminal
C       CALL FINITT(0,760)
C       NOW FIND COEFFS OF OBSERVED DATA ↑↑↑↑↑↑↑↑↑↑↑↑↑↑↑↑↑↑↑↑↑↑↑↑↑↑↑↑↑↑↑↑↑↑↑
        PI=3.1415926535
        WRITE(5,*)' '
C       The following is used if the Delta Pressure Step is desired output
C       WRITE(5,*)'      DPS           NP(J)'
C       MAX M IS NO. OF FOURIER COEFFS
        DO 106 M=1,10
C       FSR IN PRESSURE UNITS
C       SRS=75.53
        SUNC=0.
        SUNS=0.
        C2=6.28318*M/SRS
        DO 107 J=1,34
        IF (J .NE. 1) GO TO 104
C       Following line calculates the difference in pressure between 1st 2 steps
        DPS=NP(J+1)-NP(J)
C       DPS=(SRS-(NP(20)-NP(1)))/2
        GO TO 105
 104    CONTINUE
C       Following line calculates the difference in pressure between steps
        DPS=NP(J)-NP(J-1)
C       IF (J .NE. 20) GO TO 105
C       DPS=(SRS-(NP(20)-NP(1)))/2
 105    CONTINUE
        IF (M .NE. 1) GO TO 116
C       The following step is used if Delta Pressure Step is desired output.
C       WRITE(5,*)DPS,NP(J)
 116    CONTINUE
C       The next two steps calculate the Fourier cos coeffs, and sin coeffs
        SUNC=SUNC+(NC(J)/M)*(2.*SIN(C2*NP(J))*((SIN(C2*DPS/2.))**2
      *)+COS(C2*NP(J))*SIN(C2*DPS))
        SUNS=SUNS+(-NC(J)/M)*(2.*COS(C2*NP(J))*((SIN(C2*DPS/2.))**2
      *)-SIN(C2*NP(J))*SIN(C2*DPS))
 107    CONTINUE
C       The next line calulates the Fourier coeffs of the fringe
        YSM(M)=SQRT(SUNS*SUNS+SUNC*SUNC)/PI
        YSCM(M)=SUNC/PI
        YSSM(M)=SUNS/PI
 106    CONTINUE
C       Following are the Fourier coeffs
        WRITE(5,*)'YSM'
        WRITE(5,*)YSM(1)
        WRITE(5,*)YSM(2)
        WRITE(5,*)YSM(3)
        WRITE(5,*)YSM(4)
        WRITE(5,*)YSM(5)
        WRITE(5,*)YSM(6)
```

```
      WRITE(5,*)YSM(7)
      WRITE(5,*)YSM(8)
      WRITE(5,*)YSM(9)
      WRITE(5,*)YSM(10)
C     WRITE(5,*)YSM(11)
C     WRITE(5,*)YSM(12)
C     WRITE(5,*)YSM(13)
C     WRITE(5,*)YSM(14)
C     WRITE(5,*)YSM(15)
C     BELOW IRRELEVANT EXCEPT FOR LASER COEFFS##########################
      WRITE(5,*)'NOW PLOT OBSERVED DATA USING FOURIER COEFFS'
      CALL INITT(30)
      CALL DWINDO(0.,629.,-1.,1.)
      CALL TWINDO(50,900,50,800)
      CALL MOVEA(0.,0.)
      X=.01
C    FIND FIRST VALUE FW AND CENTRAL CW TO N PLOT ONLY
C     FW=YSM(1)*COS(.01/100)+YSM(2)*COS(2*.01/100)
C    *+YSM(3)*COS(3*.01/100)+YSM(4)*COS(4*.01/100)
C    *+YSM(5)*COS(5*.01/100)+YSM(6)*COS(6*.01/100)
C    *+YSM(7)*COS(7*.01/100)+YSM(8)*COS(8*.01/100)
C     CW=YSM(1)*COS(PI)+YSM(2)*COS(2*PI)+YSM(3)*COS(3*PI)
C    *+YSM(4)*COS(4*PI)+YSM(5)*COS(5*PI)+YSM(6)*COS(6*PI)
C    *+YSM(7)*COS(7*PI)+YSM(8)*COS(8*PI)+YSM(9)*COS(9*PI)
 900  Y=((YSM(1)*COS(X/100)+YSM(2)*COS(2*X/100)+YSM(3)*COS(3*X/100)
     *+YSM(4)*COS(4*X/100)+YSM(5)*COS(5*X/100)+YSM(6)*COS(6*X/100)
     *+YSM(7)*COS(7*X/100)+YSM(8)*COS(8*X/100)+YSM(9)*COS(9*X/100)
     *+YSM(10)*COS(10*X/100)+YSM(11)*COS(11*X/100)
     *+YSM(12)*COS(12*X/100)+YSM(13)*COS(13*X/100)
     *+YSM(14)*COS(14*X/100)+YSM(15)*COS(15*X/100)))
C910  CALL DRAWA(X,Y)
      X=X+1
C     IF (X .LE. 629) GO TO 900
C     NOW PLOT LASER PROFILE WITH FOURIER COEFFS
      X=.01
      REAL L(10)
C     LASER COEFFS FOR FSR OF 75.7332 PSI
      L(1)=.2254809
      L(2)=.1613598
      L(3)=.1071364
      L(4)=.094267033
      L(5)=.074299119
      L(6)=.055807292
      L(7)=.029683163
      L(8)=.02819389
      L(9)=.018680153
      L(10)=.018559434
C     200++++++++++++++++++++++++++++++++++++++++++++++++++++++++++++++++++
C     LASER FIRST VALUE (LF), LASER CENTRAL VALUE (LC) TO N PLOT ONLY
C     FF=.7633933
C     CC=-0.1496794
C920  Y=((L(1)*COS(X/100)+L(2)*COS(2*X/100)+L(3)*COS(3*X/100)
```

```
 920  Y=L(1)*COS(X/100)+L(2)*COS(2*X/100)+L(3)*COS(3*X/100)
     *+L(4)*COS(4*X/100)+L(5)*COS(5*X/100)
     *+L(6)*COS(6*X/100)+L(7)*COS(7*X/100)
     *+L(8)*COS(8*X/100)+L(9)*COS(9*X/100)
     *+L(10)*COS(1C .X/100)
CCC   CALL DRAWA(X,Y)
      X=X+1
CCC   IF (X .LE. 629) GO TO 920
C     ****************************************************************
C     10 Fourier coeffs were found but any number up to 10 may be used
C     Now select the number of Fourier coeffs to be used:
C     YSM(3)=0.
C     YS.(4)=0.
C     YSM(5)=0.
C     YSM(6)=0.
      YSM(7)=0.
      YSM(8)=0.
      YSM(9)=0.
      YSM(10)=0.
C     PLOT CONVOLUTED PROFILE
      CALL MOVEA(0.,0.)
      DO 940 M=1,10
C     DECONVOLUTE LASER FROM OBSERVED DATA (/20 NORMALIZES ONLY)
 940  YSM(M)=(YSM(M)/L(M))/20
      WRITE(5,*)'DECONVOLUTED COEFFS ARE'
      WRITE(5,*)YSM(1)
      WRITE(5,*)YSM(2)
      WRITE(5,*)YSM(3)
      WRITE(5,*)YSM(4)
      WRITE(5,*)YSM(5)
      WRITE(5,*)YSM(6)
      WRITE(5,*)YSM(7)
      WRITE(5,*)YSM(8)
      WRITE(5,*)YSM(9)
      WRITE(5,*)YSM(10)
      WRITE(5,*)'THIS TEXT CAUSES LAST LINE TO PRINT
C     TO AVERAGE COEFFS WITH ANOTHER PROFILE JJJJJJJJJJJJJJJJJJJJJJJ
C     C1=8.738/100
C     C2=4.583/100
C     C3=2.346/100
C     YSM(1)=(YSM(1)+C1)/2
C     YSM(2)=(YSM(2)+C2)/2
C     YSM(3)=(YSM(3)+C3)/2
C     WRITE(5,*)'AVERAGE COEFFS ARE'
C     WRITE(5,*)YSM(1)
C     WRITE(5,*)YSM(2)
C     WRITE(5,*)YSM(3)
C     JJJJJJJJJJJJJJJJJJJJJJJJJJJJJJJJJJJJJJJJJJJJJJJJJJJJJJJJJJJJJJJJ
C     ****************TO PLOT LASER PROFILE INSTEAD***
C     YSM(1)=.2433401
C     YSM(2)=.1676189
C     YSM(3)=.1367357
```

```
C     ***********************************************
      X=.01
C     FIRST PLOT IS NON NORMALIZED VERSION
 950  Y=YSM(1)*COS(X/100)+YSM(2)*COS(2*X/100)+YSM(3)*COS(3*X/100)
     *+YSM(4)*COS(4*X/100)
     *+YSM(5)*COS(5*X/100)
     *+YSM(6)*COS(6*X/100)+YSM(7)*COS(7*X/100)+YSM(8)*COS(8*X/100)
CC    CALL DRAWA(X,Y)
C     WRITE(5,*)'X,Y'
C     WRITE(5,*)X,Y
C     FIND FIRST AND CENTRAL VALUES TO NORMALIZE IN STEP 980
      IF (X .NE. .01) GO TO 960
      FV=Y
 960  IF (X .NE. 315.01) GO TO 970
C     WRITE(5,*)'X IS 315 X AND Y ARE'
C     WRITE(5,*)X,Y
C     WRITE(5,*)'*****************'
      CV=Y
C     WRITE(5,*)'CENTRAL VALUE IS CV='
C     WRITE(5,*)CV
C     WRITE(5,*)'*****************'
 970  X=X+1
      IF (X .LE. 629) GO TO 950
      WRITE(5,*)'FIRST VALUE, FV, CENTRAL VALUE, CV'
      WRITE(5,*)FV,CV
C     WRITE(5,*)'CV IS'
C     WRITE(5,*)CV
      WRITE(5,*)'THIS TEXT CAUSES LAST LINE TO PRINT'
      CO=(15.689416*((SRS/(2*PI))**2))/10000
      WRITE(5,*)'CO'
      WRITE(5,*)CO
      WRITE(5,*)'%%%%%%%%%%%%%%%%%%%%%%%%%%%%%%%%%%%%%%%%%%%%%%'
      CALL MOVEA(0,0.)
C     CALL DRAWA(629.,0.)
C     CALL MOVEA(0.,.2)
C     CALL DRAWA(629.,.2)
C     CALL MOVEA(0.,.4)
C     CALL DRAWA(629.,.4)
C     CALL MOVEA(0.,.5)
C     CALL DRAWA(629.,.5)
C     CALL MOVEA(0.,.6)
C     CALL DRAWA(629.,.6)
C     CALL MOVEA(0.,.8)
C     300++++++++++++++++++++++++++++++++++++++++++++++++++++++++++++++++
C     CALL DRAWA(629.,.8)
C     CALL MOVEA(0.,1.)
C     CALL DRAWA(629.,1.)
C     NOW PLOT NORMALIZED CONVOLUTED DATA
      CALL DWINDO(-315.,315.,0.,1.)
      X=.01-315.
 980  Y=((YSM(1)*COS((X/100))+YSM(2)*COS(2*X/100)
     *+YSM(3)*COS((3*X/100))
```

```
     *+YSM( 4 )*COS( 4*X/100 )
     *+YSM( 5 )*COS( 5*X/100 )
     *+YSM( 6 )*COS( 6*X/100 )
     *+YSM( 7 )*COS( ( 7*X/100 ) )+YSM( 8 )*COS( 8*X/100 )
     *+YSM( 9 )*COS( 9*X/100 )+YSM( 10 )*COS( 10*X/100 )
     * )-CV )/( FV-CV )
      CALL DRAWA( X,Y )
C     WRITE( 5,* )X,Y
      X=X+1
      IF ( X .LE. 315 ) GO TO 980
C     PLOT THREE REFERENCE CURVES T=800,1200,1600
      CALL MOVEA( 0.,1. )
C     Following is temperature of first reference curve
      T=800
 984  X=0.
      CALL MOVEA( 0.,1. )
C     Below is the theoretical gaussian fringe profile
 985  Y=EXP( -CO*( X*X )/T )
      CALL DRAWA( X,Y )
      X=X+10
C     In the following line 315 is used because pi radians of fringe plotted
      IF ( X .LE. 315 ) GO TO 985
      T=T+400
      IF ( T .LE. 1600 ) GO TO 984
C     FIND SQUARE ERROR FOR T=
C     Start searching for correct temperature at the temperature below
      T=400
      WRITE( 5,* )'TEMP, ERROR'
 986  ER=0.
      X=0.
 987  ER=ER+( ( ( ( ( YSM( 1 )*COS( ( X/100 ) )+YSM( 2 )*COS( 2*X/100 )
     *+YSM( 3 )*COS( ( 3*X/100 ) )+YSM( 4 )*COS( 4*X/100 )
     *+YSM( 5 )*COS( ( 5*X/100 ) )+YSM( 6 )*COS( 6*X/100 )
     *+YSM( 7 )*COS( ( 7*X/100 ) )+YSM( 8 )*COS( 8*X/100 )
     *+YSM( 9 )*COS( 9*X/100 )+YSM( 10 )*COS( 10*X/100 )
     * )-CV )/( FV-CV ) )-
     *( EXP( -CO*( X*X )/T ) ) )**2 )
      X=X+10
      IF(  X .LE. 315. ) GO TO 987
C     WRITE( 5,* )'TEMP, ERROR'
      WRITE( 5,* )T,ER
C     WRITE( 5,* )'THIS TEXT CAUSES LAST LINE TO PRINT'
      T=T+10
      IF ( T .LE. 1700 ) GO TO 986
      CLOSE( UNIT=3,DISPOSE='SAVE' )
C     Next line applies to graphing on terminal
      CALL FINITT( 0,760 )
      END
```

```
.TYPE G.COM

      FORTRAN/LIST:FW2:G.LST/SHOW:3 G.G
      LINK G/LINKLIBRARY:FSPLIB
      R G
```

```
Gu

.

.       FORTRAN/LIST:FW2:G.LST/SHOW:3 G.G
.MAIN.

.       LINK G/LINKLIBRARY:FSPLIB
?LINK-W-Undefined globals:
$VIRSZ

.       R G
ZW   ZS
↑↑↑↑↑↑↑↑↑↑↑
BACKGROUND INTENSITY IS
  988.7231
  75.53000
NC BEFORE NORMALIZING AND AFTER SUBTRACTION OF BG
  41.25928
  136.7249
  11.27686
  120.3678
  72.98279
  119.8583
  125.0291
  413.9391
  433.7892
  816.1156
  1174.443
  1839.478
  2851.599
  4722.567
  6891.408
  8991.732
  10968.37
  11536.11
  11110.94
  9288.200
  6731.890
  4509.587
  2715.975
  1797.112
  918.6843
  663.2294
  319.3577
  169.7096
  303.6644
  149.3887
  141.9388
  114.2964
  104.1340
 -41.25934
```

WX IS
11536.11
PRESSURE, COUNTS, KILORAYLEIGHS, IN RAW DATA FORM
LAST 2 COLUMNS ARE NEW PRESSURE AND NEW COUNTS

PL	CL	KL	NP NC	
957.1900	584.0000	0.5670000	960.7752	3.5765325E-03
954.9500	628.0000	0.5580000	958.5333	1.1851901E-02
952.7000	555.0000	0.5550000	956.2716	9.7752654E-04
950.3500	610.0000	0.5500000	953.9160	1.0434001E-02
948.1900	585.0000	0.5510000	951.7607	6.3264635E-03
946.2000	633.0000	0.5710000	949.7921	1.0389834E-02
943.8500	656.0000	0.5890000	947.4012	1.0838059E-02
941.6300	843.0000	0.6010000	945.1664	3.5882030E-02
939.2400	872.0000	0.6130000	942.7611	3.7602723E-02
937.3100	1119.000	0.6200000	940.8429	7.0744425E-02
934.8000	1339.000	0.6190000	938.3013	0.1018058
932.5200	1745.000	0.6170000	936.0159	0.1594539
930.6400	2381.000	0.6200000	934.1635	0.2471890
928.0900	3541.000	0.6200000	931.5568	0.4093725
925.7500	4799.000	0.6090000	929.2112	0.5973770
923.8500	6128.000	0.6140000	927.3290	0.7794423
921.5500	7246.000	0.6060000	925.0110	0.9507859
919.3300	7565.000	0.6040000	922.7765	1.000000
917.4700	7163.000	0.5920000	920.9374	0.9631442
914.9400	6012.000	0.5850000	918.3515	0.8051413
912.7600	4532.000	0.5870000	916.1726	0.5835493
910.6800	3255.000	0.5920000	914.0910	0.3909105
908.3000	2208.000	0.5960000	911.6835	0.2354324
906.3900	1652.000	0.5930000	909.7880	0.1557814
904.0000	1133.000	0.5940000	907.3646	7.9635531E-02
901.9500	973.0000	0.5890000	905.3192	5.7491589E-02
899.3400	777.0000	0.5940000	902.6629	2.7683303E-02
897.0800	680.0000	0.5870000	900.4006	1.4711161E-02
895.0400	747.0000	0.5780000	898.3924	2.6322946E-02
892.6400	651.0000	0.5720000	895.9683	1.2949656E-02
890.3300	649.0000	0.5740000	893.6648	1.2303872E-02
888.2900	621.0000	0.5630000	891.6171	9.9077048E-03
885.7800	612.0000	0.5600000	889.0557	9.0267882E-03
883.5200	523.0000	0.5520000	886.7994	-3.5765378E-03

THIS TEXT CAUSES LAST LINE TO PRINT
SRS
75.53000

YSM
0.3696032
0.2238235
0.1115526
4.6207257E-02
1.6699495E-02
5.2267537E-03
1.8393536E-03
1.2564364E-03

```
 3.5860834E-03
 3.0901073E-03
ROW@PLOT OBSERVED DATA USING FOURIER COEFFS



7  @



DECONVOLUTED COEFFS ARE
 8.1958868E-02
 6.9355413E-02
 5.2061040E-02
 2.4508704E-02
 1.1238017E-02
 4.6828589E-03
 0.0000000
 0.0000000
 0.0000000
 0.0000000
THIS TEXT CAUSES LAST LINE TO PRINT
FIRST VALUE, FV, CENTRAL VALUE, CV
 0.2438049      -4.6711199E-02
THIS TEXT CAUSES LAST LINE TO PRINT
CO
 0.2267180
ZZZBZZZRRRZRRSZRZNNRBRZBBXBXZXZZBBXBZDEBBHZKBLMwOPQxST!:#TyUWzXZ([\!↑_)$@~BC DF"
`GaHJbKLcNdOFeRSfUVsWhYZi[]J↑_J%AKBC1EFGImJ"m%JKMNOQRTUVXYZ\1]↑1&@KABDJEFiHIhJLsM
OfFeQSdTcUWbXaY`[\! ]~_)'@A:C(D!('DzEGyHxJwKLvNuOPtRsSTrUr*PPtQvSxTzU!W X"aYd[s\J
↑n_a+@uByC)D#aFeG#e+GJHoJtKyL N$eOKPaRwS~T%eV1WsY(Z&b[J]s↑(_'d,A1BuC E(hFrG(I)eJP
KzM)z,M*dNoOzQ+eRPT(U,fVaX!Y-hZs\ ].J↑v-@/bAmByDOdEPF(H1fIrJ)L2hMsN)P3hQ3h-QrS)T4
sUPWzX5cY1[u\~]6f_n.@vA)C7dDKEaGwH!I8bKfLKNoOrPvRxS(T)V~W X8 .X9`Z[\8 ↑~_)/@(BxCu
DrFoGKIfJaK7!MwNaOJQdR6)SvUnVfW5~YuZ1[c]4z↑P_4P/_fOA3!BrChE2)FrHhI1)JaLfMO(NoPdQ/
xRmTaU.vVJX- YsZh\,!]a↑f1@+zAoCdD+d1D*yEoGdH)zIoKeL((MaOhP'~QuS1TcU&(WrXJYb[%z\s↑
1_e2@$~BwCaDkFeG# HyJ#y2JtKoLJNeOaP")RySuTaVnWJXsZd[a]! ↑!_z3AxBvCtErFr6AsBCtDuFG
vHwJKxM!x6MyNzOQ(R!S)UV~W Y"`Z[a]b↑c_c7AdBeCEfFsHIhJLiMNJPQKRTU1VXYmZ\]↑m8@A"m8AB
DEGHIKL1MOFQKSTJUWXiY[h\]s_f9@BeCDdFGcHbJKaLN`O! PR~ST)V!WX(Z[z]!z9]↑y_y!AxBCwEFG
vIJuKMNOtQRSUsVWYZ\]r↑r;@ABDEFHr<BC9`.[[[8K/H6PV6P/V3wOCOoQ-c↑*`1L'mY%12G#~T"~3BJ
O! ]x4JuXs5ESr6@N[r7IVr8DQ_r9LZr!GU!r!Ur;BP]9`.[[8r/H7iV5KOC2!QO↑↑-n1L*(Y(r2G&tT%
c3B#~Oc]"a4JdX!)5ExS!x5Su6@tNs[r7IVr8DQ_r9LZr!GUr;BP]9`.[[8u/H7wV6fOC4hQ2`↑/t1L-i
Y+a2G
```

TEMP.	ERROR
400.0000	0.2097060
410.0000	0.1945095
420.0000	0.1801474
430.0000	0.1665846
440.0000	0.1537879
450.0000	0.1417260
460.0000	0.1303690
470.0000	0.1196891
480.0000	0.1096597
490.0000	0.1002555
500.0000	9.1452442E-02
510.0000	8.3228029E-02
520.0000	7.5560570E-02
530.0000	6.8429396E-02
540.0000	6.1815027E-02
550.0000	5.5698719E-02
560.0000	5.0062709E-02
570.0000	4.4890013E-02
580.0000	4.0164385E-02
590.0000	3.5870302E-02
600.0000	3.1992738E-02
610.0000	2.8518166E-02
620.0000	2.5432343E-02
630.0000	2.2722503E-02
640.0000	2.0376189E-02
650.0000	1.8381432E-02
660.0000	1.6726822E-02
670.0000	1.5401303E-02
680.0000	1.4394365E-02
690.0000	1.3695851E-02
700.0000	1.3296020E-02
710.0000	1.3185506E-02
720.0000	1.3355302E-02
730.0000	1.3796733E-02
740.0000	1.4501466E-02
750.0000	1.5461468E-02
760.0000	1.6668990E-02
770.0000	1.8116590E-02
780.0000	1.9797074E-02
790.0000	2.1703515E-02
800.0000	2.3829229E-02
810.0000	2.6167762E-02
820.0000	2.8712889E-02
830.0000	3.1458605E-02
840.0000	3.4399092E-02
850.0000	3.7528761E-02
860.0000	4.0842198E-02
870.0000	4.4334162E-02
↑C880.0000	4.7999568E-02

↑C

TYPE 0.0

```
C      PROG TO READ AND MODIFY LASER PROFILES
C      TEMP(LASER) PRESSURE(LASER) COUNTS(LASER)
       DIMENSION YSM(35),YSCM(35),YSSM(35)
       REAL TL(130)
       REAL PL(130)
       REAL CL(130)
       REAL NP(130)
       REAL NC(68)
       OPEN(UNIT=3,NAME='FW2:FP11.DAT',READONLY,TYPE='OLD')
       WRITE(5,*)'    TL              NP                   CL              NC'
       DO 100 I=1,68
       READ(3,50) TL(I),PL(I),CL(I)
       IF (I .LE. 4 ) GO TO 100
C      START TEMPERATURE COMPENSATION
C      NEW PRESSURE (NP)=PRESSURE OF LASER(PL)*TEMP FACTOR
       NP(I)=PL(I)*(298./(273.+TL(I)))
C      NORMALIZE THE COUNTS
       NC(I)=CL(I)/32350
       WRITE(5,*)TL(I),NP(I),CL(I),NC(I)
50     FORMAT (9X,F6.3,F7.2,15X,F6.0)
100    CONTINUE
C      NOW SMOOTH THE LASER SCAN USING FOURIER/ROBLE METHOD
       PI=3.1415926535
       WRITE(5,*)'NP AT 1,2,3,4,5'
       WRITE(5,*)NP(1)
       WRITE(5,*)NP(2)
       WRITE(5,*)NP(3)
       WRITE(5,*)NP(4)
       WRITE(5,*)NP(5)
       WRITE(5,*)'NP AT 68,69'
       WRITE(5,*)NP(68)
       WRITE(5,*)NP(69)
       NP(1)=NP(5)
       NP(20)=NP(68)
       NP(2)=NP(17)
       NP(3)=NP(19)
       NP(4)=NP(21)
       NP(5)=NP(23)
       NP(6)=NP(25)
       NP(7)=NP(27)
       NP(8)=NP(29)
       NP(9)=NP(31)
       NP(10)=NP(33)
       NP(11)=NP(35)
       NP(12)=NP(37)
```

```
      NP(13)=NP(39)
      NP(14)=NP(41)
      NP(15)=NP(43)
      NP(16)=NP(45)
      NP(17)=NP(47)
      NP(18)=NP(49)
      NP(19)=NP(51)
      W=1
      WRITE(5,*)'NEW PRESSURE VALUES NP'
 103  WRITE(5,*)W,NP(W)
      W=W+1.
      IF (W .LE. 20) GO TO 103
      DO 106 M=1,21
C     FSR IN PRESSURE UNITS
C     SRS=53.2464
C     SRS=43.3838
      SRS=75.5332
      SUNC=0.
      SUNS=0.
      C2=6.28318*M/SRS
      DO 107 I=5,68
      IF (I .NE. 5 ) GO TO 104
      DPS=NP(I+1)-NP(I)
      GO TO 105
104   CONTINUE
      DPS=NP(I)-NP(I-1)
105   CONTINUE
      IF (M .NE. 1) GO TO 116
CC    WRITE(5,*)DPS
CC    WRITE(5,*)NP(I)
116   CONTINUE
      SUNC=SUNC+(NC(I)/M)*(2.*SIN(C2*NP(I))*((SIN(C2*DPS/2.))**2
     *)+COS(C2*NP(I))*SIN(C2*DPS))
      SUNS=SUNS+(-NC(I)/M)*(2.*COS(C2*NP(I))*((SIN(C2*DPS/2.))**2
     *)-SIN(C2*NP(I))*SIN(C2*DPS))
107   CONTINUE
      YSM(M)=SQRT(SUNS*SUNS+SUNC*SUNC)/PI
      YSCM(M)=SUNC/PI
      YSSM(M)=SUNS/PI
106   CONTINUE
      WRITE(5,*)'YSM'
      WRITE(5,*)YSM(1)
      WRITE(5,*)YSM(2)
      WRITE(5,*)YSM(3)
      WRITE(5,*)YSM(4)
      WRITE(5,*)YSM(5)
      WRITE(5,*)YSM(6)
      WRITE(5,*)YSM(7)
      WRITE(5,*)YSM(8)
      WRITE(5,*)YSM(9)
```

```
      WRITE(5,*)YSM(10)
      WRITE(5,*)YSM(11)
      WRITE(5,*)YSM(12)
      WRITE(5,*)YSM(13)
      WRITE(5,*)YSM(14)
      WRITE(5,*)YSM(15)
      WRITE(5,*)YSM(16)
      WRITE(5,*)YSM(17)
      WRITE(5,*)YSM(18)
      WRITE(5,*)YSM(19)
      WRITE(5,*)YSM(20)
      WRITE(5,*)YSM(21)
      CALL INITT(30)
      CALL DWINDO(0.,629.,-1.,1.)
      CALL TWINDO(50,900,50,800)
      CALL MOVEA(0.,0.)
      X=.01
900   Y=YSM(1)*COS(X/100)+YSM(2)*COS(2*X/100)+YSM(3)*COS(3*X/100)+YSM(4)
     **COS(4*X/100)+YSM(5)*COS(5*X/100)+YSM(6)*COS(6*X/100)+YSM(7)*COS
     *(7*X/100)
     *+YSM(8)*COS(8*X/100)
     *+YSM(9)*COS(9*X/100)+YSM(10)*COS
     *(10*X/100)
CC    *+YSM(11)*COS(11*X/100)+YSM(12)*COS(12*X/100)
C    *+YSM(13)*COS(13*X/100)+YSM(14)*COS(14*X/100)+YSM(15)*COS(15*X/100)
C    *+YSM(16)*COS(16*X/100)+YSM(17)*COS(17*X/100)+YSM(18)*COS(18*X/100)
C    *+YSM(19)*COS(19*X/100)+YSM(20)*COS(20*X/100)+YSM(21)*COS(21*X/100)
C     IF (X .GE. 2) GO TO 910
      WRITE(5,*)'X,Y'
      WRITE(5,*)X,Y
 910  CALL DRAWA(X,Y)
      X=X+1
      IF (X .LE. 629) GO TO 900
      CLOSE(UNIT=3,DISPOSE='SAVE')
      CALL FINITT(0,760)
      END


.TYPE O.COM

      FORTRAN/LIST:FW2:O.LST/SHOW:3 O.O
      LINK O/LINKLIBRARY:FSPLIB
      R O


.@O
```

```
.       FORTRAN/LIST:FW2:O.LST/SHOW:3 O.O
.MAIN.

.       LINK O/LINKLIBRARY:FSPLIB
?LINK-W-Undefined globals:
$VIRSZ

.       R O
   TL               NP                   CL               NC
?Err 5
in   routine ".MAIN."  line 10


?Err 5
in   routine ".MAIN."  line 10


  23.77200        939.0898        3509.000        0.1084699
  23.88800        940.5798        3409.000        0.1053787
  23.99800        941.9172        3434.000        0.1061515
  24.10500        943.1827        3317.000        0.1025348
  24.21600        944.3544        3374.000        0.1042968
  24.31800        945.4337        3304.000        0.1021329
  24.44800        946.3330        3333.000        0.1030294
  24.64100        946.7205        3189.000        9.8578051E-02
  24.72700        947.6982        3211.000        9.9258117E-02
  24.77300        948.9128        3386.000        0.1046677
  24.81400        950.1931        3363.000        0.1039567
  24.84900        951.4221        3287.000        0.1016074
  24.88700        952.6312        3385.000        0.1046368
  24.97300        953.2164        3454.000        0.1067697
  24.99300        954.5724        3323.000        0.1027202
  25.02300        955.7662        3642.000        0.1125811
  25.05100        956.8363        3622.000        0.1119629
  25.06800        957.8914        3722.000        0.1150541
  25.07500        959.3185        3837.000        0.1186090
  25.08100        960.7289        4064.000        0.1256260
  25.10700        961.6247        4104.000        0.1268624
  25.11100        963.1113        4476.000        0.1383617
  25.11600        964.4546        4941.000        0.1527357
  25.12700        965.7284        5274.000        0.1630294
  25.12900        967.0714        5498.000        0.1699536
  25.13400        968.3645        6284.000        0.1942504
  25.14800        969.1286        6991.000        0.2161051
  25.14300        970.1844        8488.000        0.2623802
  25.13200        971.5097        11030.00        0.3409583
  25.12700        972.7354        16357.00        0.5056260
  25.12600        974.1281        24998.00        0.7727357
  25.12400        975.5840        32280.00        0.9978362
  25.12700        976.8936        32312.00        0.9988254
```

25.14000	977.7606	28974.00	0.8956414
25.14000	979.2099	22393.00	0.6922102
25.14600	980.5896	16566.00	0.5120866
25.15100	981.8824	12226.00	0.3779289
25.15600	983.2053	9171.000	0.2834930
25.15900	984.4948	7474.000	0.2310355
25.16800	985.0446	6617.000	0.2045441
25.16500	986.5237	5754.000	0.1778671
25.16200	987.8430	5349.000	0.1653478
25.15800	988.9757	4901.000	0.1514992
25.15800	990.1851	4684.000	0.1447913
25.16000	991.4576	4362.000	0.1348377
25.16000	992.7970	4224.000	0.1305719
25.15200	993.5732	4035.000	0.1247295
25.15100	994.8059	3970.000	0.1227202
25.14900	996.0220	3882.000	0.1200000
25.14500	997.3847	3711.000	0.1147141
25.14300	998.7208	3633.000	0.1123029
25.14100	999.9669	3773.000	0.1166306
25.14200	1000.813	3606.000	0.1114683
25.13800	1002.316	3611.000	0.1116229
25.13900	1003.622	3613.000	0.1116847
25.14200	1004.941	3541.000	0.1094590
25.14500	1006.290	3732.000	0.1153632
25.15300	1007.503	3567.000	0.1102628
25.15700	1008.749	3707.000	0.1145904
25.15800	1009.565	3607.000	0.1114992
25.15800	1011.004	3609.000	0.1115611
25.16200	1012.160	3605.000	0.1114374
25.15600	1013.529	3551.000	0.1097682
25.14300	1014.623	3434.000	0.1061515

```
NP AT 1,2,3,4,5
 0.0000000
 0.0000000
 0.0000000
 0.0000000
  939.0898
NP AT 68,69
  1014.623
 0.0000000
NEW PRESSURE VALUES NP
  1.000000       939.0898
  2.000000       952.6312
  3.000000       954.5724
  4.000000       956.8363
  5.000000       959.3185
  6.000000       961.6247
  7.000000       964.4546
```

```
  8.000000        967.0714
  9.000000        969.1286
  10.00000        971.5097
  11.00000        974.1281
  12.00000        976.8936
  13.00000        979.2099
  14.00000        981.8824
  15.00000        984.4948
  16.00000        986.5237
  17.00000        988.9757
  18.00000        991.4576
  19.00000        993.5732
  20.00000        1014.623
YSM
 0.2254809
 0.1613598
 0.1071364
 9.4267033E-02
 7.4299119E-02
 5.5807292E-02
 2.9683163E-02
 2.8193893E-02
 1.8680153E-02
 1.8559434E-02
 4.4040936E-03
 9.1322120E-03
 4.7645955E-03
 7.8142360E-03
 4.0516402E-03
 2.6422290E-03
 5.1584304E-04
 2.9768483E-03
 3.2191928E-03
 3.7323066E-03
 1.9601721E-03
X,Y
 9.9999998E-03  0.8134672
X,Y
  1.010000       0.8127617
X,Y
  2.010000       0.8106764
X,Y
  3.010000       0.8072207
X,Y
  4.010000       0.8024113
X,Y
  5.010000       0.7962701
X,Y
  6.010000       0.7888262
X,Y
  7.010000       0.7801136
X,Y
  8.010000       0.7701731
X,Y
  9.010000       0.7590501
X,Y
  10.01000       0.7467955
X,Y
  11.01000       0.7334650
X,Y
7 12.01000       0.7191188
```

APPENDIX E. SHADOW HEIGHT

Shadow Height in Two Dimensions

To explain the concept of shadow height, this section shows how shadow height is calculated for the simplified case of two dimensions.

The first step is to find:

M = distance from observer to shadow along line of observations from α and θ, where

α = angle from local vertical to line of observation, where positive values are toward the Sun, and

θ = change in latitude between observer and sunset as shown.

M is found in terms of α and θ. Then, shadow height will be found in terms of M and α.

Let $\beta \equiv \alpha - \theta$, $h \equiv M \cos\beta$

$$M = \frac{h}{\cos \beta} = \frac{h}{\cos (\alpha-\theta)} = \frac{r - r \cos\theta}{\cos (\alpha-\theta)}$$

which applies for $\alpha \pm 90°$.

Shadow height (SH) is determined from M and α (see Figure E-1), using the cosine law, where $\Psi \equiv 90 - |\alpha|$

$$(SH + r)^2 = r^2 + M^2 - 2rM \cos (90 + \Psi)$$

$$SH + r = [r^2 + M^2 - 2rM \cos (90 + \Psi)]^{\frac{1}{2}}$$

$$SH = [r^2 + M^2 - 2rM \cos (90 + \Psi)]^{\frac{1}{2}} - r$$

$$SH = [r^2 + M^2 - 2rM \cos |\alpha|]^{\frac{1}{2}} - r$$

because $\cos(90 + \Psi) = \cos(90 + (90 - |\alpha|))$

$$= \cos(180 - |\alpha|)$$

$$= -\cos|\alpha|$$

Shadow Height Program Rotations Used

Two shadow height programs are included. One of these programs (L.SH) is a simple version, but it requires the solar depression angle T1, and the azmuth (or bearing, i.e., E from N) angle from the Sun of the observation be input (in degrees). These two angles may not be known, but they are not required in the more complex version of the program (M.SH). Instead, the time and place are input and these two angles are calculated in M.SH. The rest of M.SH is the same as program L.SH.

The components of the vector from the Earth to the Sun in "inertial space" are found in M.SH. This vector is called VI. By performing a series of rotations, this vector is transformed into the frame of the observer, so the resulting vector VL gives the direction to the Sun from the observer in terms of local zenith and azmuth.

To demonstrate this, an example is shown below. In Figure E-2 the components of VI are X, Y, and Z. With an angle of 66° for ϕ, these components are 0, 0.9, and 0.4, respectively. The next rotation produces the "Geographic Vector," VG, which is fixed with respect to Earth and points toward the Sun. The amount of rotation, -GSTR, depends on the time.

The next rotation is the longitude rotation. If the observer is at the 0° longitude, in England, as he is in this example, the rotation is 0.

The next rotation is the latitude rotation. Here, the coordinate system is rotated 90° about Y; then the coordinate system is rotated through an angle that equals latitude, so the Z axis is in the local vertical. The X axis points south and the Y axis points east. As in the other rotations, the new components for the unit vector pointing to the Sun in this rotated coordinate frame are computed. These new vector components are VL(1), VL(2), and VL(3).

Finally, the observer has the components of a unit vector pointing toward the Sun in terms of local zenith, south, and east, so he can easily calculate the zenith and bearing angles to the Sun. The zenith angle; i.e., the angle from the zenith to the Sun is

$$\phi = \tan^{-1} \frac{\sqrt{y^2 + x^2}}{z} ,$$

which can be visualized by translating the XY plane component along Z to the maximum Z value.

To find the bearing, or azimuth angle,

$$\theta = \tan^{-1} \frac{y}{x}$$

is computed, where θ is measured to the E from S. To convert this to a "bearing" angle which is defined as angle E of N,

$$\text{Azimuth} = \text{Bearing} = 180 - \theta$$

TABLE E-1. SHADOW HEIGHT PROGRAM VECTOR COMPONENTS

	X	Y	Z	
VI	0	0.9	0.4	inertial vector
VG	0.9	0	0.4	geographic vector
VJ	0.9	0	0.4	after longitude rotation
VL	0.05	0	0.95	after latitude rotation

Shadow Height Programs

```
TYPE M.SH
C      m.sh SHADOW HEIGHT PROG. BASED ON LOCAL TIME
       DIMENSION VI(3),BV(3),VG(3),VL(3),VJ(3),PV(3),ZZ(3,3)
       DIMENSION C(3,3),CT(3,3)
       CALL INITT(30)
       CALL DWINDO(7200 ,67000.,0.,250.)
       CALL TWINDO(50,900,50,800)
       CALL MOVEA(0.,0.)
       CALL MOVEA(3600.,0.)
       CALL DRAWA(3600.,10.)
       CALL MOVEA(7200.,0.)
       CALL DRAWA(7200.,0.)
       RAD=57.295779
C      LATITUDE AND LONGITUDE OF OBSERVER IS
       ALA=64.86001/RAD
       ALO=-147.84711/RAD
C      ALA=49./RAD
C      ALO=-122./RAD
       IDAY=61
C      IDAY=46
       IYR=1984
    3  SECS=0.
       CALL MOVEA(0.,0.)
C   4  WRITE(5,*)'ENTER YEAR (INTEGER), DAY (INTEGER), SECONDS (REAL)'
    4  MS=1
C      ################
C      ↑↑↑↑↑↑↑↑↑↑↑↑↑↑↑
C   5  READ(5,*)   IYR,IDAY,SECS
       IF (IYR.LT.1901.OR.IYR.GT.2099) STOP
       CALL SUN(IYR,IDAY,SECS,GST,SLONG,SRASN,SDEC)
C      WRITE(5,200)
C      WRITE(5,300) IYR,IDAY,SECS,GST,SLONG,SDEC
C      GO TO 5
COO    FORMAT(2I4,F10.2)
200    FORMAT(8X,'IYR',6X,'IDAY',6X,'SECS',7X,'GST',5X,'SLONG',
      *5X,'SDEC')
300    FORMAT(1X,2I10,4F10.3)
C      ***********************************************************
C      NOW FIND INERTIAL COORDS (VI) FROM SDEC AND SLONG
       P=((3.141592/2)-(SDEC/RAD))
       SLONG=SLONG/RAD
       VI1=SIN(P)*COS(SLONG)
       VI2=(SIN(P)*SIN(SLONG))
       VI3=COS(P)
       VI(1)=VI1
       VI(2)=VI2
       VI(3)=VI3
C      WRITE(5,*)'INERTIAL VECTOR VI X Y Z COMPS ARE'
C      WRITE(5,*)VI
C      **************************************************************
C      NOW TRANSFORM THE INERTAIL COORDINATES (VI) TO GEOGRAPHIC (VG)
       GSTR=GST/RAD
       CALL ROTXYZ(-GSTR,ZZ,3)
```

```
      CALL TRF(VI,ZZ,VG)
C     WRITE(5,*)' GEOGRAPHIC VECTOR VG X Y Z COMPS TO SUN FROM EARTH'
C     WRITE(5,*)VG
C     ******************************** ******************************
C     NOW TRANSFORM THE GEOGRAPHIC COORDS (VG) TO LOCAL AZIMUTH AND ZENITH
C NEXT ROTATE LONG ABOUT Z AXIS
      XI=90./RAD
      CALL ROTXYZ(-ALO,ZZ,3)
      CALL TRF(VG,ZZ,VJ)
C     WRITE(5,*)' VJ IS'
C     WRITE(5,*)VJ
C NEXT ROTATE LAT, AND 90 DEGREES ABOUT Y
      E=-ALA+XI
      CALL ROTXYZ(E,ZZ,2)
      CALL TRF(VJ,ZZ,VL)
C     WRITE(5,*)'ZENITH FROM ACOS Z TO SUN IS '
      X=VL(1)
      Y=VL(2)
      Z=VL(3)
      SQ=SQRT((X**2)+(Y**2))
      AZ=(ATAN2(SQ,Z))*RAD
C     WRITE(5,*)AZ
      TH=(ATAN2(Y,X))*RAD
      B=180-TH
C     WRITE(5,*)'AZIMUTH TH IS'
C     WRITE(5,*)TH
C     WRITE(5,*)'BEARING TO SUN IS'
C     WRITE(5,*)B
C     ### NOW FIND  SHADOW HEIGHT################################
C     FIND SOLAR DEPRESSION ANGLE
      TI=AZ-90.
C     TI=45.
C     WRITE(5,*)'SOLAR DEPRESSION ANGLE IS'
C     WRITE(5,*)TI
C     INPUT GEOGRAPHIC BEARING ANGLE OF OSERVATION
C     WRITE(5,*)'INPUT GEOGRAPHIC BEARING ANGLE OF OBS (DEG)'
C     READ(5,*)GB
      GB=.01
C     WRITE(5,*)'======================================'
COO   WRITE(5,*)'GEOGRAPHIC BEARING ANGLE OF OBS IS'
C     WRITE(5,*)GB
900   MS2=1
C     INPUT ENITH OF OBSERVTION (DEGREES)
C     WRITE(5,*)'INPUT ZENITH OF OBS'
C     READ(5,*)ZI
      ZI=60.
C     WRITE(5,*)'ZENITH OF OBSERVATION IS '
C     WRITE(5,*)ZI
C     CALCULATE BEARING ANGLE OF OBSERVATION FROM SUN
910   SI=GB-B
C     SI=45.
C     WRITE(5,*)'BEARING ANGLE OF OBSERVATION FROM SUN IS'
C     WRITE(5,*)SI
```

```
C       NOW RUN SHADOW HEIGHT PROG L.SH
C       Z=ZENITH ANGLE, S=AZIMUTH, T=SOLAR DEPRESSION ANGLE
C       RADIUS OF EARTH IS KM IS:
        RA=6378.
C       THE FOLLOWING 3 VALUES ARE INPUTS TO PROG (ABOVE)
C       ZI IS ZENITH INPUT (DEGREES) OF OBSERVATION
C       SI IS AZIMUTH INPUT (DEGREES) BEARING ANGLE FROM SUN OF OBSERVATION
C       TI IS SOLAR DEPRESSION ANGLE INPUT (DEGREES)
C       NOW CONVERT THESE TO RADIANS:
        Z=ZI/RAD
        S=SI/RAD
        T=TI/RAD
        C1=1/((SIN(T))**2)
        C2=(((COS(Z))**2)*((COS(T))**2))/(((SIN(Z))**2)*((SIN(T))**4))
        C3=(2*COS(Z)*COS(T)*COS(S))/(SIN(Z)*((SIN(T))**3))
        C4=(COS(T)*COS(S))/SIN(T)
        C5=COS(Z)/(((SIN(T))**2)*SIN(Z))
        C6=C4+C5+((C1+C2+C3)**.5)
        AP=(SIN(Z)*C6)-(COS(Z))
        P=RA/AP
        AG=(((RA**2)+(P**2)+(2*RA*P*(COS(Z))))**.5)-RA
C       WRITE(5,*)'HEIGHT ABOVE GROUND IS'
C       WRITE(5,*)AG
        GB=GB+90.
C       WRITE(5,*)'===================='
        IF (GB .EQ. 90.01) GO TO 950
        IF (GB .EQ. 270.01) GO TO 955
        IF (GB .EQ. 360.01) GO TO 960
        IF (GB .EQ. 450.01) GO TO 970
        GO TO 1000
950     S2=AG
        GO TO 1010
955     S1=AG
        GO TO 1010
960     W1=AG
        GO TO 1010
970     S4=AG
        GO TO 1020
1000    S3=AG
1010    IF(GB .LT. 280) GO TO 900
C       NOW ZENITH OBSERVATION
        ZI=0.01
        GO TO 910
C       WRITE IN ORDER OF N E S W ZENITH
C020    WRITE(5,*)S2,S3,S1,W1,S4
1020    LL=1.
        IF (SECS .GT. 61200.) GO TO 2000
        IF (SECS .LT. 10800.) GO TO 2000
        CALL DRAWA (SECS,S4)
2000        SECS=SECS+1200.
        IF(SECS .LT. 86400.) GO TO 4
        IDAY=IDAY+8
C       WRITE(5,*)'DAY'
```

```
C     WRITE(5,*)IDAY
      GO TO 3
      CALL FINITT(0,760)
      END

.TYPE M.COM
      FORTRAN/LIST:FW2:M.LST/SHOW:3 M.SH
      LINK M,ALL11/LIBRARY:FSPLIB
      R M

.TYPE SUN.CAL
        SUBROUTINE SUN(IYR,IDAY,SECS,GST,SLONG,SRASN,SDEC)
        DATA RAD /57.29578/
        DOUBLE PRECISION DJ,FDAY
        IF(IYR.LT.1901.OR.IYR.GT.2099) RETURN
        FDAY=SECS/86400.
        DJ=365*(IYR-1900)+(IYR-1901)/4+IDAY+FDAY-0.5D0
        T=DJ/36525.
        VL=DMOD(279.696678+0.9856473354*DJ, 360.D0)
        GST=DMOD(279.690983+0.9856473354*DJ+360.*FDAY+180., 360.D0)
        G=DMOD(358.475845+0.985600267*DJ, 360.D0)/RAD
        SLONG=VL+(1.91946-0.004789*T)*SIN(G)+0.020094*SIN(2.*G)
        OBLIQ=(23.45229-0.0130125*T)/RAD
        SLP=(SLONG-0.005686)/RAD
        SIND=SIN(OBLIQ)*SIN(SLP)
        COSD=SQRT(1.-SIND**2)
        SDEC=RAD*ATAN(SIND/COSD)
        COTAN=COS(OBLIQ)/SIN(OBLIQ)
        SRASN=180.-RAD*ATAN2(COTAN*SIND/COSD,-COS(SLP)/COSD)
        RETURN
        END
```

```
      SUBROUTINE TRF(X,A,XT)
      DIMENSION X(3),A(3,3),XT(3)
      DO 1 I=1,3
      XT(I)=0.0
      DO 1 J=1,3
      XT(I)=XT(I)+A(I,J)*X(J)
1     CONTINUE
      RETURN
      END
       SUBROUTINE ROTXYZ(A,B,IROT)
       DIMENSION B(3,3)
       A1=COS(A)
       A2=SIN(A)
       GO TO (1,2,3),IROT
C       ROTATION ABOUT THE X-AXIS
1      B(1,1)=1.0
       B(1,2)=0.0
       B(1,3)=0.0
       B(2,1)=0.0
       B(2,2)=A1
       B(2,3)=-A2
       B(3,1)=0.0
       B(3,2)=A2
       B(3,3)=A1
       RETURN
C       ROTATION ABOUT THE Y-AXIS
2      B(1,1)=A1
       B(1,2)=0.0
       B(1,3)=-A2
       B(2,1)=0.0
       B(2,2)=1.0
       B(2,3)=0.0
       B(3,1)=A2
       B(3,2)=0.0
       B(3,3)=A1
       RETURN
C       ROTATION ABOUT THE Z-AXIS
3      B(1,1)=A1
       B(1,2)=-A2
       B(1,3)=0.0
       B(2,1)=A2
       B(2,2)=A1
       B(2,3)=0.0
       B(3,1)=0.0
       B(3,2)=0.0
       B(3,3)=1.0
       RETURN
       END
```

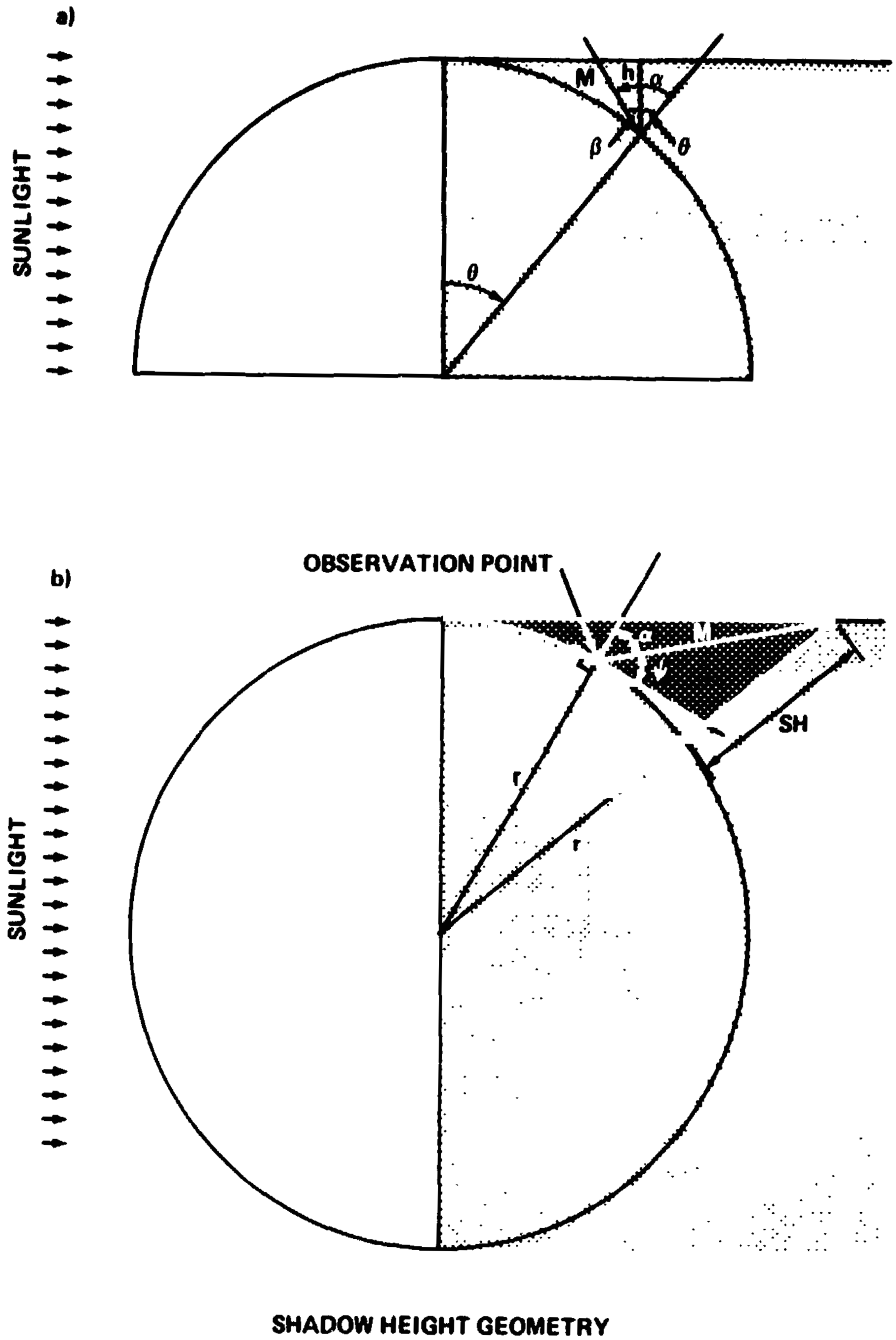

Figure E-1. Local shadow height geometry.

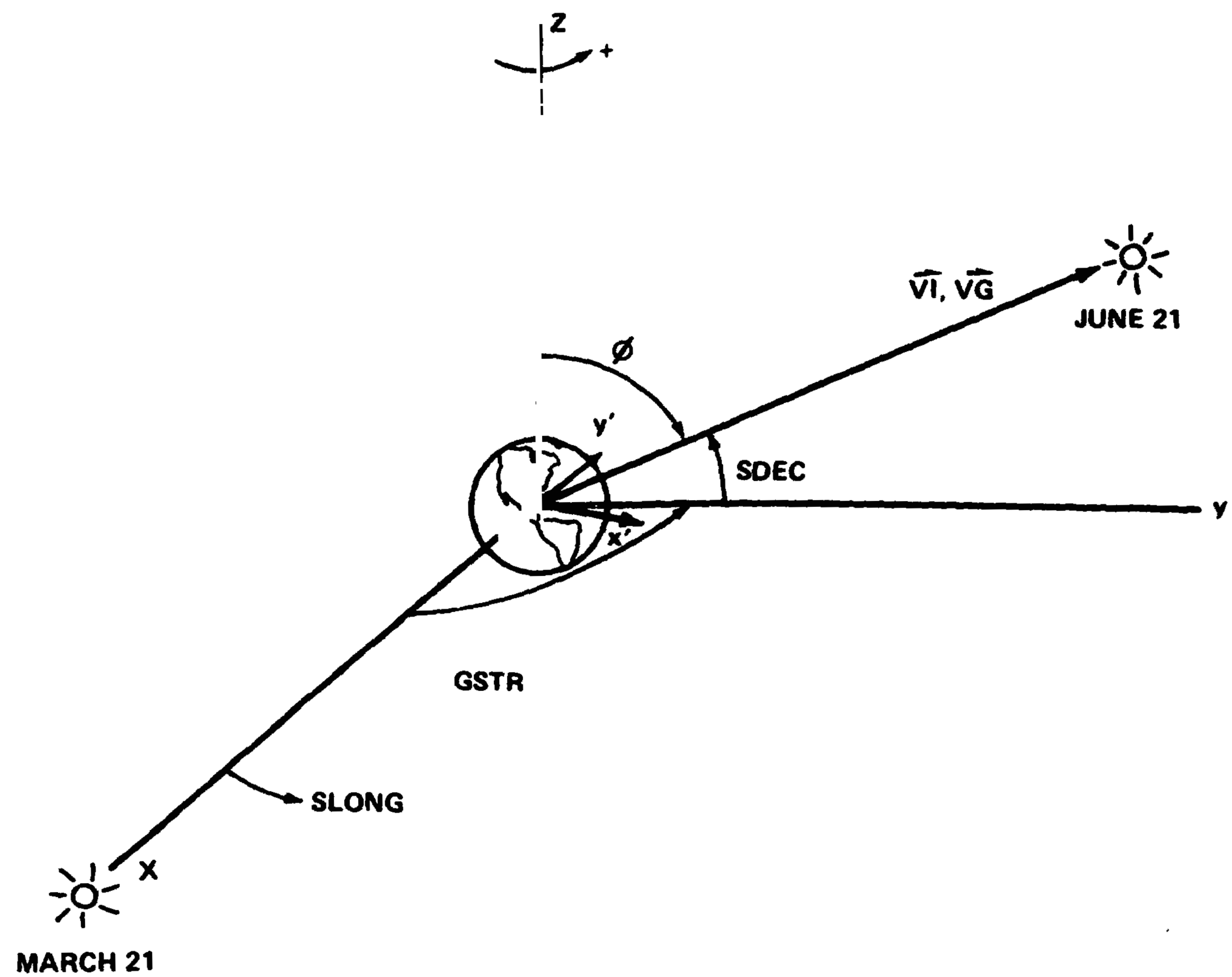

Figure E-2. Global geometric parameters used in shadow height program.

APPENDIX F. EXAMPLE OF RAW DATA

Scan Number		T,°C		Pressure	Encoder Position		Counts	Photometer							Mirror Position
3	34	24	246	897.79	3876	0	456	0	206	0	0	0000	0	0	1
3	35	24	248	899 89	3968	-3	476	0	206	0	0.0000		0	0	1
3	36	24	245	902 33	4058	0	530	0	203	0	0	0000	0	0	1
3	37	24	248	904 67	4150	143	691	0	211	0	0	0000	0	0	1
3	38	24	251	906 85	4240	0	763	0	203	0	0	0000	0	0	1
3	39	24	240	908 46	4330	9	1087	0	205	0	0	0000	0	0	1
3	40	24	247	911 79	4420	6	1347	0	210	0	0	0000	0	0	1
3	41	24	254	914 02	4510	3	1664	0	213	0.	0	0000	0	0	1
3	42	24	251	916 51	4600	-3	2013	0	214	0	0	0000	0	0	1
3	43	24	250	918 92	4690	3	2172	0	212	0	0	0000	0	0	1
3	44	24	250	920 89	4778	-3	2065	0	211	0	0	0000	0	0	1
3	45	24	240	923 32	4864	-3	1754	0	215	0	0	0000	0	0	1
3	46	24	229	925 82	4952	12	1438	0	215	0	0	0000	0	0	1
3	47	24	242	928 33	5040	137	1096	0	218	0	0	0000	0	0	1
3	48	24	250	930 42	5124	0	835	0	213	0	0	0000	0	0	1
3	49	24	243	932 99	5210	6	656	0	214	0	0	0000	0	0	1
3	50	24	246	935 17	5292	6	627	0	212	0	0	0000	0	0	1
3	51	24	241	937 18	5376	-3	498	0	211	0	0	0000	0	0	1
3	52	24	242	939 55	5458	-3	514	0	215	0	0	0000	0	0	1
3	53	24	235	942 09	5542	3	492	0	211	0	0	0000	0	0	1
3	54	24	240	944 49	5624	-3	437	0	210	0	0	0000	0	0	1
3	55	24	239	946 89	5704	15	417	0	218	0	0	0000	0	0	1
3	56	24	236	948 87	5784	-6	437	0	218	0	0	0000	0	0	1
3	57	24	228	951 23	5862	3	454	0	213	0	0	0000	0	0	1
3	58	24	227	953 86	5942	125	412	0	217	0	0	0000	0	0	1
3	59	24	235	956 00	6024	-3	409	0	215	0	0	0000	0	0	1
3	60	24	191	958 33	6104	-3	385	0	215	0	0	0000	0	0	1
3	61	24	198	961 14	6184	3	435	0	217	0	0	0000	0	0	1
3	62	24	225	963 36	6264	-6	474	0	217	0	0	0000	0	0	1
3	63	24	226	965 85	6342	0	468	0	221	0	0	0000	0	0	1
3	64	24	228	967 97	6418	3	430	0	221	0	0	0000	0	0	1

SCAN AT TIME 94956 PERISCOPE AZ AND EL 0 00 0 00 FOR/BACK 1

4	65	24	174	967 70	6420	-6	449	0	227	0	0	0000	0	0	1
4	66	24	162	964 65	6344	-6	438	0	231	0	0	0000	0	0	1
4	67	24	141	961 94	6266	-121	441	0	234	0	0	0000	0	0	1
4	69	24	099	959 66	6188	0	448	0	238	0	0	0000	0	0	1
4	89	24	070	957 59	6110	-6	458	0	245	0	0	0000	0	0	1
4	70	24	077	955 10	6032	0	469	0	250	0	0	0000	0	0	1
4	71	24	072	952 75	5952	0	414	0	252	0	0	0000	0	0	1
4	72	24	063	950 31	5872	-6	499	0	249	0	0	0000	0	0	1
4	73	24	069	947 69	5792	-3	430	0	254	0	0	0000	0	0	1
4	74	24	059	945 43	5712	-3	441	0	244	0	0	0000	0	0	1
4	75	24	057	943 18	5630	-3	496	0	250	0	0	0000	0	0	1
4	76	24	057	941 01	5548	0	479	0	2:2	0	0	0000	0	0	1
4	77	24	070	938 32	5464	-3	503	0	246	0	0	0000	0	0	1
4	78	24	063	936 10	5380	-6	582	0	242	0	0	0000	0	0	1
4	79	24	068	933 47	5298	-6	664	0	239	0	0	0000	0	0	1
4	80	24	063	931 01	5210	-134	872	0	234	0	0	0000	0	0	1
4	81	24	057	928 77	5126	3	1103	0	236	0	0	0000	0	0	1
4	82	24	051	926 63	5040	-3	1428	0	240	0	0	0000	0	0	1
4	83	24	067	924 20	4954	-134	1881	0	242	0	0	0000	0	0	1
4	84	24	065	921 94	4870	3	2234	0	242	0	0	0000	0	0	1
4	85	24	059	919 70	4784	-3	2502	0	242	0	0	0000	0	0	1
4	86	24	069	917 21	4698	-134	2414	0	233	0	0	0000	0	0	1
4	87	24	065	914 99	4612	3	2246	0	233	0	0	0000	0	0	1
4	89	24	060	913 03	4526	-6	1771	0	240	0	0	0000	0	0	1
4	89	24	079	910 42	4438	-6	1358	0	237	0	0	0000	0	0	1
4	90	24	077	908 08	4346	0	1019	0	235	0	0	0000	0	0	1
4	91	24	072	905 73	4256	-9	848	0	227	0	0	0000	0	0	1

APPENDIX G. VERIFICATION OF EQUATION (A-1), APPENDIX A

We can find the temperature T in terms of width by substituting $\frac{1}{2}$ I_{max} for I in equation (A-1)

$$\text{where } I_{max} = \left\{\frac{M_c^{\;2}}{2\pi kT\lambda_o^2}\right\}^{1/2}$$

Substituting into equation (A-1) gives:

$$\tfrac{1}{2}\left\{\frac{M_c^{\;2}}{2\pi kT\lambda_o^2}\right\}^{1/2} = \left\{\frac{M_c^{\;2}}{2\pi kT\lambda_o^2}\right\}^{1/2} \exp\left\{\frac{-M_c^{\;2}}{2kT\lambda_o^2}(\Delta\lambda)^2\right\}$$

Solving for T, we obtain:

$$\ln(\tfrac{1}{2}) = \frac{-2.196825683 \times 10^{26}}{T}(\Delta\lambda)^2$$

$$T = 3.169349519 \times 10^{26} \; (\Delta\lambda)^2$$

where $\Delta\lambda$ is the HWHM in meters.

To input Å rather than m, we have:

$$T = 3.169349519 \times 10^{6} \; (\Delta\lambda)^2$$

where $\Delta\lambda$ is the HWHM specified in Å.

To put the formula in terms of FWHM, multiply the numerical constant by $(\frac{1}{2})^2 = \frac{1}{4}$

$$T = 7.92337 \times 10^5 \, (\Delta\lambda)^2$$

where $\Delta\lambda$ is the FWHM in Å.

This is consistent with the result of Wark [3] who obtained $T = 7.89 \times 10^5$ $(\Delta\lambda)^2$. To find a characteristic value for $\Delta\lambda$, we solve for HWHM (Å) from above:

$$(\Delta\lambda)^2 = \frac{T}{3.16 \times 10^6}$$

$$\text{HWHM (Å)} = \Delta\lambda = \frac{T}{3.16 \times 10^6}$$

For $T = 1000$ K, HWHM (Å) $= 0.01776$

$= 17.76$ mÅ

APPROVAL

AURORAL THERMOSPHERE TEMPERATURES FROM OBSERVATIONS OF 6300 Å EMISSIONS

By John C. Bird, Gary R. Swenson, and Richard H. Comfort

The information in this report has been reviewed for technical content. Review of any information concerning Department of Defense or nuclear energy activities or programs has been made by the MSFC Security Classification Officer. This report, in its entirety, has been determined to be unclassified.

A. J. DESSLER
Director, Space Science Laboratory

☆ U.S. GOVERNMENT PRINTING OFFICE 1985—631-058/20052